Analytical description of the forming process of a double curvature shipbuilding plate

J. van Cappellen

SBP-500
Nieland
PWP-100

TU Delft

Analytical description of the forming process of a double curvature shipbuilding plate

by

J. van Cappellen

to obtain the degree of Master of Science
at the Delft University of Technology,
to be defended publicly on July 19, 2021 at 14.00h.

Student number:	4364503	
Project duration:	May 5, 2020 – July 19, 2021	
Thesis committee:	Dr. C. L. Walters,	TU Delft, supervisor
	Dr. Ir. J. F. J. Pruyn,	TU Delft
	Wei Jun Wong,	TU Delft

An electronic version of this thesis is available at `http://repository.tudelft.nl/`.

Abstract

The forming of double curvature shipbuilding steel plates is performed by experienced craftsmen at IHC Metalix. Their experience will get lost when they retire; therefore, it can be valuable for future metal workers to capture the forming process of a double curved plate theoretically. An analytical description and understanding of the forming process will help craftsmen. In the future, it could even lead to the development of automatic forming machines.

This research investigates plastic deformation initiated by a rolling and a three-point bending machine forming a saddle shaped plate. A 2D-optimization for the three-point bending process is performed using beam theory. A single bend is validated by a 2D Finite Element Analysis (FEA). The rolling process is analytically described by equations obtained from literature. These equations are used to find a relation between the material stretching/membrane strains and the rolling forces. Furthermore, an elastic-perfectly plastic stress-strain curve is used. Material hardening and residual stresses due to repeated bending or rolling operations are not taken into account.

The bending optimization resulted in the least number of bending operations needed over a cross-section, assuming the cross-section behaves like a beam. The rolling equations resulted in required rolling forces for a desired membrane strain. The craftsmen know by experience that bending operations should be performed first to initiate a first curvature. Thereafter, the plate is rolled to initiate the second curvature and form the saddle shape.

In this thesis, the first steps are taken to capture and predict the manual forming process of double curvature steel plates. Future work on this topic should take the 3D-effects of the three-point bending into account which lead to more accurate analytical descriptions. Furthermore, other assumptions could be analyzed to get better understanding of their contribution.

Preface

This report is conducted to complete a Master's degree in Marine Technology at the Delft University of Technology. The last year I worked on modeling the forming process of a double curvature shipbuilding plate. The results from this thesis will give machine operators a better insight in the forming process of a plate. This thesis can be seen as a framework in more research related to the forming process of a double curvature plate.

This study could not have been completed without the help and support of several people. In the first place, I would like to thank Carey Walters for the great guidance throughout my whole research. You learned me to work in a structured way and to stay motivated by using your experience as a supervisor. In the end, you even helped me finding a job! Secondly, I would like to thank IHC for the insight in the forming processes, the data on the machines, and example geometry. Also, I would like to thank my committee members, Jeroen Pruyn and Wei Jun Wong for their assessment of the work.

Last but not least, I would like to thank my family and friends. Starting with my friends from "structures verticale 1" group, for all the online coffee breaks, motivation and concentration during the Covid times. I finally would like to thank my family and girlfriend for their encouragement throughout the process.

J. van Cappellen
Delft, July 2021

Contents

List of Tables **ix**

List of Figures **xi**

Nomenclature **xiii**

1 Introduction **1**
- 1.1 Background 1
- 1.2 Problem Statement 2
- 1.3 Investigated Plate Bending Methods 3

2 Literature Review **5**
- 2.1 Geometrical Mapping 5
- 2.2 Double Curvature Forming Research 6
- 2.3 Spring Back 8
- 2.4 Residual Stresses 10
- 2.5 Hardening 11
- 2.6 Research Gap 13
- 2.7 Methodology 14

3 Current Practice **15**
- 3.1 Double Curved Plate 15
  - 3.1.1 Membrane strains 16
  - 3.1.2 Bending Strains 17
- 3.2 Forming Processes 17

4 Three Point Bending **19**
- 4.1 Single Bend 19
  - 4.1.1 Support Distance 21
  - 4.1.2 Von Mises Criterion 23
- 4.2 FEA verification 24
  - 4.2.1 Plastic Hinge 25
  - 4.2.2 Support Distance 26
  - 4.2.3 Analytical Force 27
  - 4.2.4 Conclusion 28
- 4.3 Bending Optimization 29
  - 4.3.1 Setup 29
  - 4.3.2 Optimization Procedure 30
  - 4.3.3 Results 30
- 4.4 Practical Relevance 32

5 Plate Rolling **33**
- 5.1 Rolling model 33
  - 5.1.1 Rolling Force 34
  - 5.1.2 Global Equilibrium 35
- 5.2 Practical Relevance 40
- 5.3 Conclusion 40

6 Conclusion and Discussion **41**
- 6.1 Conclusion 41
- 6.2 Discussion and Recommendations 42

Bibliography **45**

List of Tables

4.1 Analytical forces for yielding and plastic moment calculated 26
4.2 Comparison of the analytical and numerical results 28
4.3 Optimization results for different setups 32

List of Figures

1.1 Bow of a vessel which displays complex double curved plates [33] 2
1.2 Visualization of three point bending on a plate [12] 2
1.3 Visualization of the rolling process on a plate [12] 2
1.4 Two main cold forming processes considered in this review 3

2.1 Plate bending with a LARS, difference between transverse and longitudinal curvature [30] 7
2.2 Multi point forming machine used in research by Hwang and Lee [10] 7
2.3 Stress-strain curve demonstrating spring back in the unloading phase 9
2.4 Thesis approach 14

3.1 A saddle and barrel shaped surface respectively 15
3.2 The initial flat plate before forming 16
3.3 The desired shape of the plate 16
3.4 The total membrane strain over the length of the plate at a certain y position 17
3.5 The total membrane strain over the width of the plate at a certain y position 17
3.6 Three point bending machine at IHC, dimensions are in millimeter [1] 18
3.7 Rolling machine at IHC, dimensions are in millimeter [1] 18

4.1 Three point bending of a beam with rectangular cross-section 19
4.2 Moment distribution and stress distribution over the thickness for a full plastic hinge . . 20
4.3 The deflection for a full plastic hinge with constant distance between supports 21
4.4 Actual bending operation supports and press 21
4.5 Contact locations of the press and support 22
4.6 The normalized deflection is plotted over the normalized distance between the two supports 23
4.7 The geometry used in FEA 24
4.8 The mesh size in the FEA simulation 25
4.9 Through thickness normal stress for a full plastic hinge 25
4.10 Through thickness normal stress obtained from the FEA 25
4.11 Difference between long and short distance of contact in ANSYS. Red is the longer and black is the shorter distance. 26
4.12 Comparison of analytical and numerical distance between the supports 26
4.13 The analytical and numerical deflection before and after spring back 27
4.14 First material yielding during the bending simulation 28
4.15 Full plastic hinge that arises during bending operation 28
4.16 Desired and initial cross-section at $x = L$ 29
4.17 Result of the first optimization from the example geometry 30
4.18 Result of the same optimization with 100 mm support distance 31
4.19 Result of the same optimization with 75 mm support distance 31

5.1 The assumed geometry based on the study by Salimi and Sassani [27] 34
5.2 Initial and desired cross-section of one edge of the example geometry, y/B = 0 35
5.3 Top view of a possible rolling line 36
5.4 Curvature over the same cross-section as in Figure 5.2, y/B = 0 36
5.5 Deflection for a part of the plate due to rolling 37
5.6 Overview of line part 37
5.7 The created shape and desired shape at y/B = 0 38
5.8 Required membrane strain for desired curvature at y/B = 0 39
5.9 Membrane strain geometrical approach and global equilibrium approach 39

Nomenclature

δ	Total deflection of the beam	mm
δ_c, δ_o	The height of the contact location between the beam and press or support	mm
ϵ_1, ϵ_2 and ϵ_3	Principal strains	-
ϵ_{yield}	The yielding strain	-
κ	Curvature	1/mm
σ_v	Von Mises Yield criterion	MPa
σ_1,σ_2 and σ_3	Principal stresses	MPa
σ_{yield}	The yielding stress	MPa
θ	Angle of the beam between the press and support	rad
E_s	Secant modulus	MPa
$F_{external}$	The external force per unit width required for a plastic hinge	N/mm
M_e	Yielding moment per unit width	N·mm/mm
M_p	Plastic moment	N·mm/mm
R_{xc}, R_{xo}	Half the length of the press and support	mm
R_{yc},R_{yo}	Height of press and support	mm
S_c, S_o	Contact length of the press and support	mm
E	Young's modulus	MPa
h	Thickness of the beam	mm
I	The moment of inertia	mm^4
L	Length between supports	mm
M(x)	The moment function	N·mm
S	Total distance between the press and support	mm

1

Introduction

In this chapter, the topic of this thesis is introduced and some background information is provided. Furthermore, a problem statement, a research question, and multiple sub-questions are defined. At last, the investigated bending methods are introduced briefly.

1.1. Background

The shipbuilding industry has become more complex over the years. Vessels, building technologies, designs, building tools and machines are currently more complex than years ago. New technologies are developed to decrease construction times and building costs. An example is the use of painting or welding robots. However, some parts of the shipbuilding industry are not yet developing over time. Such a niche of the industry is the forming process of double curved plates.

A ship's hull consists of many plates that are welded together. These plates can be in a planar shape, a single curvature plate or a double curvature shape. The double curvature plate is a plate bent over both its length and width axes. Each of these mentioned plate shapes are present in a vessel. Planar plates are found in the 'side hull', single curvature plates are found in the bilge and double curvature plates are found in the bow, bulb and stern of a vessel. In Figure 1.1, the bow of a vessel can be found with uniquely shaped plates. Approximately ten per cent of the ship's hull weight is originated from double curvature plates. Each double curvature hull plate is formed to its desired shape individually, this is a time consuming process. Costs can be decreased by automating the forming processes of a double curvature plate. A first step to automation will be understanding the forming process of double curvature plates.

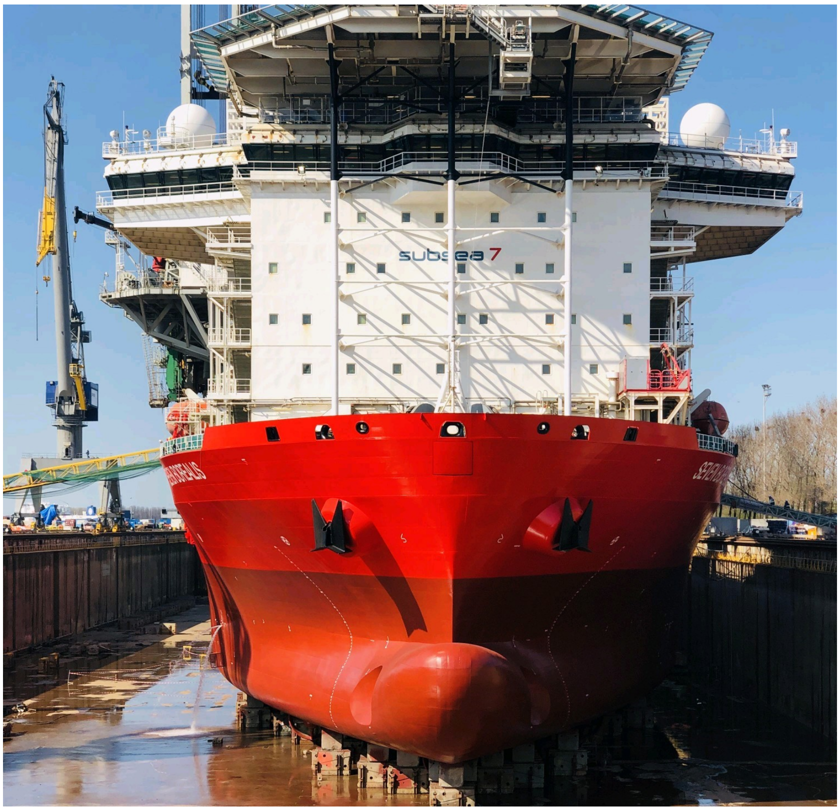

Figure 1.1: Bow of a vessel which displays complex double curved plates [33]

Currently, an experienced metal worker forms a double curvature plate through an iterative process of forming and then checking the shape against a template. The worker is basing the forming process on his years of experience in forming complex-shaped plates. A problem arises when these craftsmen retire in the near future. Their knowledge in how to form a flat plate into the right shape will be lost. In this report, an investigation into the theory behind the forming of a double curved plate is done. This leads to a prediction of the steps that need to be taken to form a desired shape from an initially flat plate. The plates are formed with three different cold forming methods: three point bending, 2 roller plate compressing and a single press machine. The research focuses on the first two mentioned processes. These two forming processes are visualized Figures 1.2 and 1.3.

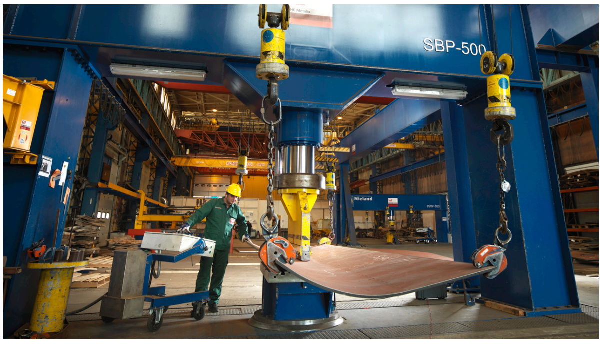

Figure 1.2: Visualization of three point bending on a plate [12]

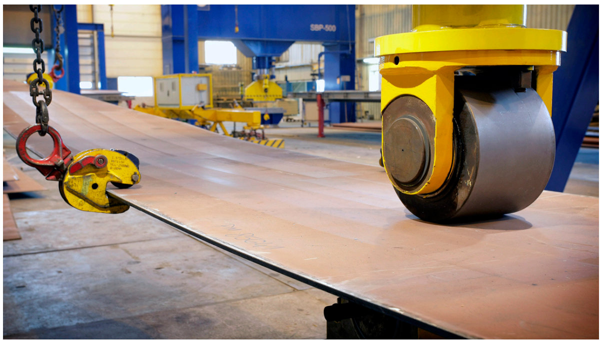

Figure 1.3: Visualization of the rolling process on a plate [12]

1.2. Problem Statement

The primary reason to look into the forming process is to save costs on the building of a vessel and to give a scientific underpinning to something that has traditionally been done with craftsmanship. This is a goal for the future. The problem statement for this thesis project will focus on the forming process of double curvature plates. If the methods of the metal worker can be adequately described, then his actions can be modeled analytically. With an analytical model, the process can be predicted which results in an instruction manual for inexperienced metal workers and ultimately in a shorter construction time. The two specific cold forming processes where this research is focused on are local processes. Next to the fact that the processes are local, the processes are repeated multiple times to obtain the desired shape. The combination of repeatedly rolling and three point bending, is one of the difficulties of this study. Prior research has been done into double curvature forming in the sheet metal industry, in a large multi-point press machines or in line rolling [30][22][23]. No research is found related to the combination of the specific forming processes. In chapter 2, literature related to this study is reviewed. Different topics that are important and related to the iterative and repeated use of forming processes are discussed. Together with the problem statement, the literature review resulted in the following research question:

How can the forming process by rolling and bending of a double curved steel shipbuilding plate be analytically modeled?

The ultimate goal is to answer the research question. To do this in a structured manner, the research question is divided in sub-questions.

- How do the two relevant bending methods (rolling and three point bending) result in curvatures of the plate?
- How can the deformations and rotations in plates analytically be modeled?
- What are the key metrics that should be optimized when evaluating a forming process?
- What are the requirements in the shipbuilding industry for the double curved steel plates, and how can these be implemented?

In the next section, a short introduction into the investigated plate bending methods is given.

1.3. Investigated Plate Bending Methods

There are multiple plate bending methods in the shipbuilding industry. The most commonly used plate bending is done by cold-forming methods. As mentioned, there are two cold forming techniques distinguished in this thesis: local three point bending (Figure 1.4a) and line rolling (Figure 1.4b). These two cold forming techniques are used to make complex double curvature plates. During this process, plastic deformation is introduced in the plate in multiple directions. Another method to form double curvature plates, is line heating. This is out of the scope of this research and therefore not investigated in detail, but a reference related to line heating is discussed briefly in the next chapter. The particular machines (seen in Figure 1.2, and Figure 1.3) and their operations are the ones this research focuses on.

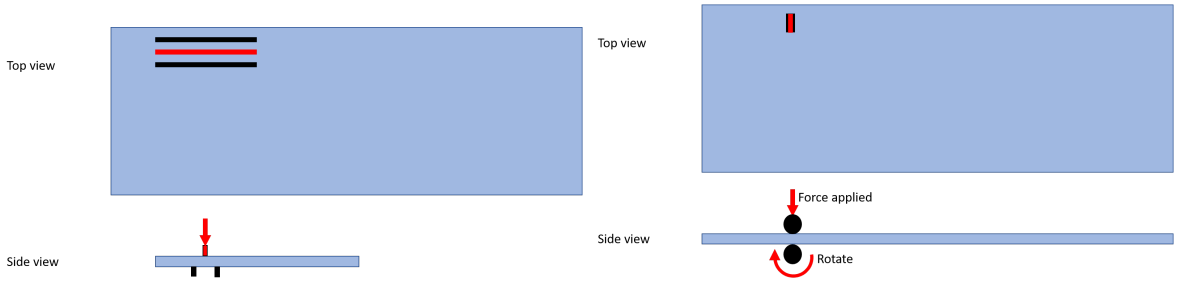

(a) Three point bending process

(b) Rolling process

Figure 1.4: Two main cold forming processes considered in this review

As can be seen in Figure 1.4, both forming processes are local processes. This makes the total forming process different from a lot of processes that are currently available. Line rolling inserts membrane strain in the rolling direction which causes a global curvature. It is called line rolling because a part smaller than the total width of the plate is rolled. The roller has a smaller width (115 mm) than the plate and so multiple lines have to be rolled to roll the whole width or length of the plate. Depending on the shape, a plate will be rolled or bent first. The three point bending process inserts bending strains which cause another curvature. As mentioned, the forming processes can be used in any desired sequence or direction. From experience, it is known that the rolling process is mainly performed in the length direction of the plate. In this direction, the longest rolling paths can be made. Therefore the operator does not have to move the plate often. The forming processes will be described individually, and it should be possible to use one process after the other.

When this view about the forming processes is sketched, a first question that arises is how to model a forming process at a certain location of the plate? This suggests that the plate can be modeled analytically with a Finite Element Method (FEM). With such a method, the stress/strain or deflection field can be calculated with a given input force. Using a FEM model to evaluate a single rolling or bending operation is possible. However, the inverse problem is a lot more difficult for such a FEM model. A simpler analytical model is sought. This brings the next question: Is it possible to analytically calculate the required input force and location of the two different processes based on the desired shape? To come to an answer of this question, more research needs to be done.

In the next chapter, a recap of the performed literature study is given. The discussion of the literature helps identifying the knowledge gap and to answer the research question.

2

Literature Review

The literature review can be divided into multiple topics related to the general findings on plate bending in the literature. First, an introduction in the investigated plate bending methods is given. These are the plate bending methods used by IHC. Hereafter, plate bending methods that are used in the shipbuilding industry are sought for. This search resulted in multiple topics. Obviously, plate deformation theories are one of the first topics that came up. However, after the literature review, it was concluded that the discussed plate theories are not applicable. Therefore, in this chapter, the plate theory section is omitted. All the discussed plate theories were elastic theories, and this thesis focuses on plasticity. Next to that, simple but accurate theories are sought for. In every deformation theory or beam theory, assumptions are made. This initiates thinking about what realistic assumptions can be made for describing the forming processes that are investigated.

One of the topics that is important in the forming process is the spring back phenomenon. The importance of this phenomena is related to the repeated, combined bending and rolling operations to form a double curved plate. Together with spring back, residual stresses and hardening of the material are important phenomena that occur in the forming process of a double curved plate. This thesis itself only takes into account spring back after bending. Material hardening and residual stresses need to be taken into account in future work on this topic. These two topics will definitely help to describe the forming processes more accurately. References related to these topics are sought to fully understand them and to find a knowledge gap related to larger shipbuilding steel plates.

Once the plate bending methods in the shipbuilding industry and the related sub topics are studied and information is gathered to make a start on an analytical model, a knowledge gap can be described. A conclusion of the literature study and scope for the practical research is given to fill this knowledge gap.

2.1. Geometrical Mapping

Curved surfaces are defined into two categories, the developable and undevelopable surfaces. A developable surface is a surface that can be formed without stretching the plate, so without changing the overall dimension. A lot of time is spent in forming these plates. To minimize the amount of strain input in the flat plate to form the desired geometry, research is done by Branco and Soares [25]. Branco and Soares are discussing a mapping method to create an associated surface that maps shell plates of a double curvature geometry into shells of a planar geometry. With this method, the lack of material or superposition of material at the connection zone between different patches give the required information to form the plates. The research shows that whenever the equation of a desired double curvature shell is not known, there is a method to calculate the required deformations of patches to acquire the desired geometry. A question that arises when this information is known is: how can the information that is found be used to form the planar plate into the double curved plate with the two forming processes? To answer this question, more information is needed about how double curvature plates can be formed with the specific forming processes. The focus of this thesis will be on the following question, how can the required strain input that is found with the mapping method [25], or a more simple difference between the initial flat plate and required geometry, be put into the material with the given forming processes?

Research by Ryu and Shin, gives an algorithm to unfold the undevelopable surfaces based on deformation theory [26]. The algorithm includes conditions for different forming methods that are used to form the plate. The algorithm focuses on minimizing the strain energy necessary to find the initial flat plate geometry. This is another a way to find the initial flat plate geometry, including the forming process conditions which makes this algorithm more complex. This is again differing from the focus of this thesis. The focus is on the forming process with a known initial geometry and desired geometry. The discussed algorithm is developed to define the flat plate dimensions. This thesis focuses on the required shape with a given initial flat plate. The initial geometry is known. This means that the mapping of a desired curved plate to a flat plate is not necessary for this thesis. However, the mapping algorithms can be used to reduce the overall forming time of a double curved plate by finding an optimal starting plate. This thesis focuses on the forming process itself, and therefore, these mapping algorithms might be helpful for future research. The next chapter will look into forming processes of double curvature plates.

2.2. Double Curvature Forming Research

In this section, different research into the general plate bending industry are given. This gives an insight into different topics that contribute to plate bending. Research into the double curvature bending of a large shipbuilding plate is done by Heo et al [8]. In this study, a flexible forming die is introduced to form differently shaped plates. The forming die is numerically modeled as well as experimentally validated. This method is created to substitute the manual line heating method. In the research, Heo et al. [8] compared the accuracy of numerical models relative to experiments. The cold forming method that is used is very different than the one this thesis focuses on. The research by Heo et al.[8] is related to the cold forming of double curvature shipbuilding plates, but it is a single step operation with a die and therefore not directly related to this thesis.

Research by Shim et al, gives an explanation about how double curvature plates are formed with a Line Array Roll Set (LARS) [30]. The forming method is different compared to the focus in this thesis. However, multiple aspects of this research are helpful for the thesis. The LARS initiates a first curvature in transverse direction by height differences between the different rollers. When the plate is put under pressure between the rollers, the first curvature is acquired. By rolling the plate a second curvature in the longitudinal direction is created, see figure 2.1. This two step process is related to the focus of this thesis. Next to that, there is information about spring back that occurs during the forming of the first curvature. The effect of initiating the second curvature on the first curvature is discussed as well. These three different aspects and their discussions are helpful for this research. They assume, for instance, elastic perfectly plastic material behaviour, which is an assumption that is often made [23] [10] [14] [19]. Next to that, the plate dimensions are closer to the dimensions this thesis is focusing on. What is different and something that this thesis is not looking for, is that the end result of the research by Shim et al. [30], are design equations that predict the curvatures of a formed shape. These equations are created with experimental coefficients.

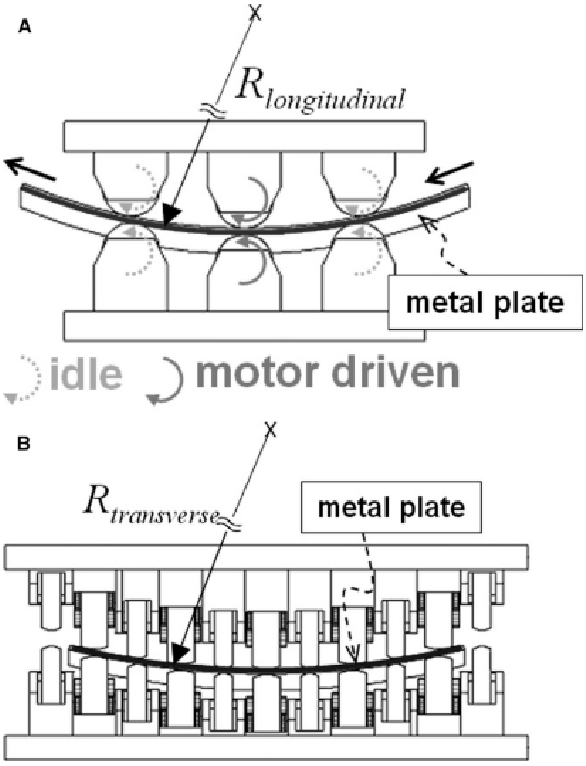

Figure 2.1: Plate bending with a LARS, difference between transverse and longitudinal curvature [30]

Another contribution related to double curvature plates is done by Hwang and Lee [10]. In this research, a double curvature plate is formed with a multi point forming press, see figure 2.2. This is a different forming method than the one this thesis focuses on. However, the discussion in the paper related to spring back compensation and taking this into account when forming the desired shape is interesting. The research uses a FEM model to iteratively find the setup that results in the smallest error between desired and shape after spring back. So, the simulation is repeated to find the optimal form of the press. This is again a different way to obtain knowledge about how to compensate for spring back. The research confirms that spring back is an important topic for plate bending. This confirms the importance of implying spring back calculations in the three point bending equations.

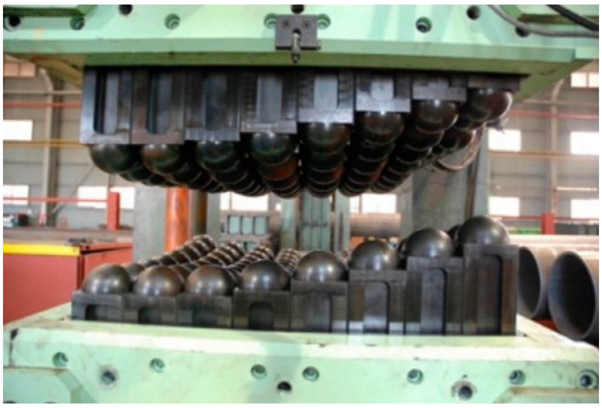

Figure 2.2: Multi point forming machine used in research by Hwang and Lee [10]

A final study that was found related to double curvature plates and the rolling forming process is done by Rady [23]. In this study, the shape change during the roll forming process is investigated. The study is focused on rolling small areas of the flat plate. This is a similarity with the focus of this thesis. The 3D forming process is decomposed into a set of 2D problems. The first one is a plane strain problem under the rollers' path. This plane strain assumption implies that the strain perpendicular to the rolling direction can be neglected. This means that the thickness reduction only results in strain into the rolling direction. This assumption is only valid whenever the rollers are far from the edges of the plate. The edge effect is also studied, whenever the rollers are close to the edge of the plate, the plate flattens again because of the plate size increase. The second 2D problem is a plane stress shell deformation. This plane stress assumption and problem is more difficult to solve. The roller forming process is considered as an eigenvalue problem. The bending equation of equilibrium under in-plane loading is given in equation 2.1.

$$D\nabla^4 w - N_{\alpha\beta} w_{,\alpha\beta} = 0 \tag{2.1}$$

where:

$D = \frac{Et^3}{12(1-\nu^2)}$ the flexural rigidity in $[\mathrm{N} \cdot \mathrm{m}^2]$
$w =$ the out of plane displacement in [mm]
$\alpha = x, y[-]$
$\beta = x, y[-]$
$N_{\alpha\beta} =$ applied force in-plane direction per unit width [N/m]

This is an eigenvalue problem because, the in-plane displacements calculated with the first 2D problem can be considered as in-plane forces. With this known, there is a non-homogeneous solution for w in Equation 2.1. These solutions can be found analytically or numerically.

The research by Rady [23] first assumed the roll forming process as a press simulation. This means that the roller movement is not taken into account, and the deformation is calculated by only assuming the pressure exerted by the rollers on the plate. This simplification is easy to compute and verify with FEA. In the recommendations, the inverse problem is introduced and a procedure is suggested to solve the inverse problem. The inverse problem is finding the forming process, given a final shape. The procedure to solve this problem starts with the representation of the desired final shape as a mapping of the original shape and the calculations of the final strain by using the incompressibility condition. The incompressibility condition in this case means that the material volumes remain constant. The strain field that will be found using this assumption is the amount of strain that needs to be put into the material while the thickness stays the same. Related to the inverse problem, Ryu [26] gives an approximated solution of the strain distribution in a plate by unfolding the desired final shape to a flat plate. This research is based on deformation theory and finite elements. In this thesis, an analytical description of the required shape and strain distribution is sought. The study by Rady [23] is helpful for modeling the roll forming process. The main issue is that there is no experimental data for validation. Next to that, a part of the study is done by FEA. While this thesis focuses on analytical solution of the forming processes. FEA will only help with a verification of the found analytical equations.

As can be seen, research is done related to double curvature plates. The references that were briefly discussed are all different in the actual forming of double curvature plates. To calculate the forces required to obtain the desired geometry of a plate, an analytical method/model is needed. The first steps into creating an analytical model are done by reviewing existing literature and obtain methods to describe the double curved plate and see which sub-topics are important to describe the forming processes mathematically. Research differing from small to large and thin to thick plates is found. These studies are related to one of the sub-topics and can therefore be found in the next sections. The sub-topics that will be discussed are spring back, residual stresses and hardening respectively. With research related to these topics an analytical model for the forming process of a double curvature plate can be established.

2.3. Spring Back

Spring back is the elastic recovery to a material that occurs when the forces on the part are released in the forming process. This can be visualised in a stress-strain curve, see figure 2.3. Spring back is an important phenomenon to take into account in the cold forming of materials. The accuracy of the end product depends on the amount of spring back that occurs. When the spring back can be calculated, this can be taken into account in the forming process. One way to compensate for spring back is the iterative repetition of the forming process. A single press does not give the desired shape. A second press is needed to compensate for the spring back as mentioned by Hwang et al[11]. Spring back is a frequent researched topic to reduce production costs and prevent inaccuracies. Below, multiple studies related to spring back are mentioned. The most interesting research is spring back related to thick steel plates and the particular forming processes.

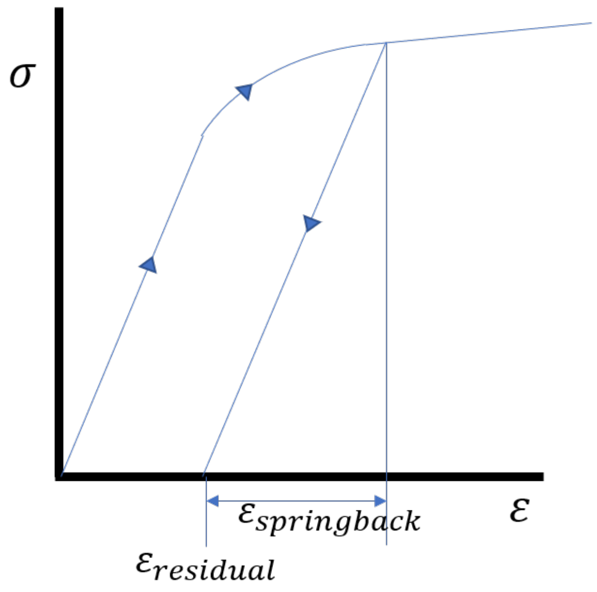

Figure 2.3: Stress-strain curve demonstrating spring back in the unloading phase

To describe spring back in an analytical model, analytical equations are sought in literature. An old investigation by Johnson and Yu gives analytical calculations for spring back [14]. The limitation to this research is the maximum deflection being less than the plate thickness which a follow up study by Johnson and Yu explained [13]. A single assumption in this research is that the material is linear elastic perfectly plastic. This is not the case if a realistic model is made but a fine assumption to be made early on in the research. As mentioned before, a elastic-perfectly plastic model is accurate and simple to use, so this will be used for the analytical model in this thesis. For a future study on this topic, the material model could be updated to a realistic stress-strain curve.

Another study into spring back and double curvature sheet metal industry is done by Parsa et al[22]. In this study, Parsa presents an analytical formulation to predict the double curvature spring back. The sheet thickness change is considered in this research. This analytical formulation is compared with numerical and experimental results. The results show that an increasing thickness and radius of curvature gives greater spring back. However, this is a different forming process (stamping) than the thesis focuses on. The influence of neutral axis shift in calculating the spring back needs to be taken into account to calculate an accurate curvature.

As mentioned, the most interesting spring back research is related to thick steel shipbuilding plates or the particular forming processes. Research related to thick shipbuilding plates is done by Shen et al [29]. In this study, the forming process with a multi-point forming mechanism, is analyzed with FEM. The effect of the curvature and plate thickness on the spring back phenomenon is discussed as well. With a different forming process to acquire a desired double curvature plate, and a numerical simulation, the study by Shen[29] is quite different from this thesis .

Borah et al did a study into spring back of a 15mm thick steel plate that is given a single curvature with a die [3]. The thickness comes closer to what this thesis is focusing on. The forming method, size of the plate, and single curvature is totally different from this thesis. Experiments are done into single curvature spring back,and double curvature spring back is investigated by FEA. This research is again suggesting that FEA is a good way to verify a particular forming process.

The studies that were discussed are the only ones that were found related to spring back in the bending of thick steel shipbuilding plates. The spring back phenomenon is a topic that is definitely needed to consider in the forming process equations. Depending on the sizes and deformations of a plate, spring back can have a large influence on the shape of the plate. To model the bending operation correctly, spring back has to be taken into account, with a simplified elastic perfectly plastic material model, the spring back phenomenon is easier to add to the model. Whenever a more complicated and realistic stress-strain curve is used, the spring back will be harder to calculate, due to hardening effects and residual stresses that are present in the material. This will be discussed in the next chapters.

2.4. Residual Stresses

This section discusses the importance of residual stresses in the material after and during the forming process. Despite that residual stresses are not used in the analytical model, this section is deliberately left in this report. The importance of residual stresses in predicting the forming process is significant, and so this section can be seen as information for future work.

Residual stresses are stress distributions that remain in the material after deforming and springing back. These stresses have influence on the cold working and final shape, especially when a location is loaded multiple times. Residual stresses are not only important for the next bending operation, they are also important for the steel strengths and therefore should be one of the results that needs to be known after the bending operation. In the research by Weng and White, a bending test of a thick plate is compared with analytical values of the residual stresses [38]. The theory that is used to calculate the residual stresses is from Dat and Peköz. In this research, the effect of strain hardening is not taken into account, and it is assumed to be fully plastic bending [4]. Basically, the residual stress is the sum of the loading and unloading stress distribution. Depending on assumptions, these stress distributions change. The unloading stress distribution is directly related to spring back of the material. These two studies show that a verification of the analytical data is necessary. The experiment is again differing with this thesis. The main message from these studies is how residual stresses are built up and that verification in any way is necessary. This applies not only to residual stresses but to the whole forming process.

In a study by Moen et al, a mathematical prediction for the residual stresses and strains is created [20]. The forming process that happens in this research is coiling a steel plate strip, uncoiling and flattening it. The study describes how the through thickness and longitudinal residuals stresses can be calculated based on multiple assumptions. For instance, some important assumptions are that the sheet thickness stays constant, the neutral axis does not shift, an elastic perfectly plastic stress-strain curve is used and plane strain behaviour is used. With these assumptions, an accurate prediction method for the through thickness, transverse and longitudinal stress distribution is created. Measurements show that the predictions are accurate at the flat sections but are over-predicting stress at the corners. However, this is a starting point to calculate residual stresses and strains in the material. The researchers suggested a way to implement a kinematic hardening rule as well. This study is one of many that uses elastic perfectly plastic material. Next to that, it is mentioned that the neutral axis does not shift. Previously, it is mentioned that the neutral axis shift is important for spring back calculations when large deflections and curvatures are initiated. Therefore, this assumption needs to be looked into for calculating accurate spring back and residual stresses.

In a study by Liu et al, a residual stress distribution is shown after multiple loading for a plate flattening process [19]. In this study, the researchers reset the residual stress to zero but kept the residual curvature, which is more important in the cold forming process. This reset gives a simpler expression for the bending moment that exists in the plate under the different rollers. The same elastic perfectly plastic material is assumed in this paper.

Research by Liu et al, compared residual stresses existing in a three point bent thick steel plate with a numerical calculation [18]. The goal of this research was to show the importance of the FEA to evaluate residual stresses in materials after cold-forming. The three point bending machine corresponds with the bending that this thesis is focused on. Therefore, the residual stress calculation of this study is useful for the cold forming at IHC. Tensile specimens were cut out of the bent plate to evaluate the mechanical properties of the material at different locations near and under the bend. The research gives more information on how residual stresses can be numerically modeled and how accurate these results are. In this thesis, this will not be very important, as the focus is on the forming process, but the effect of residual stresses on a next bend should be taken into account to accurately model the process. A verification with FEA software is helpful, as can be seen in this research.

To summarize all the important assumptions that are made in different studies:

- Maintaining the same steel sheet thickness before and after bending
- The neutral axis remains constant before and after bending
- An elastic-perfectly plastic stress-strain behaviour is used

These assumptions are valid to use as can be seen in the different studies. Whenever the verification or validation of an analytical model is not accurate, these assumptions are the first to look into. The accuracy of the model can improve if these assumptions are more realistic.

To capture the residual stress distribution of a plate, the stress distribution under loading in the different directions should be known. Whenever this stress distribution is known, an elastic stress distribution, in all directions, is subtracted, and the residual stress distribution is found. This relates back to beam and plate theories, and the models to calculate plate deformations. With an analytical formulation, FEA will help with validating the residual stress distribution after a single operation.

As can be seen in the mentioned references, the influence of residual stress on the subsequent forming process is important. Next to the influence on the forming process, residual stresses do effect the ultimate strength of the material. Based on the research by Weng and White [38], and Liu et al [18], the magnitude of residual stresses in bent plates is around maximum of 50% of the yield stress after a single bend. When the bend increases to 90 degrees , the residual stress on the inside of the curve was 92% of the yield stress [37]. These magnitudes show the importance of residual stress predictions in the plate.

In the next section, material hardening will be discussed. This is another important topic that came forth from the early literature review.

2.5. Hardening

This section discusses the importance of material hardening during the forming process. Despite that a material hardening law or rule is not used in the analytical model, this section is deliberately left in this report. The importance of material hardening in predicting the forming process is significant, and so this section can be seen as information for future work.

Hardening of steel is the increase of yield stress due to cold work which makes it harder to plastically deform the material. Hardening of the material depends on the load history of the material and can be different for both longitudinal and transverse axis. Hardening is important in the double curvature forming process of steel plates. Whenever a plate is bent at a single place, the material hardens at this place. This affects the material properties and the next bend in all directions. To be able to model the forming process, a hardening rule/model needs to be implemented. Before being able to describe the material hardening, the stress-strain relationship of the material has to be known. It is important to know that there are different models/rules to describe the hardening stress-strain relationship. In before mentioned references, the assumption of an elastic perfectly plastic material is frequently used. This indicates that a realistic stress-strain relationship is not needed to analytically model the forming processes. However, to have knowledge about the different hardening stress-strain relationships, some of them will be discussed.

In a study by Baltov and Sawczuk, a hardening rule is defined for anisotropy that is produced by plastic deformation on an initially isotropic material [2]. In this study, the difference between kinematic and isotropic hardening is highlighted and explained as well. This difference is the shift of the yield surface in kinematic hardening, while in isotropic hardening the yield surface stays at its position but increases in size. This means that when the tensile yield strength increases in kinematic hardening, the compressive yield strength decreases. In isotropic, both the tensile and compressive yield strength increase with the same amount. Kinematic hardening is also called the Bauschinger effect. Whenever the rolling and three point bending process are following up on each other, the material will be put under tension and compression in different directions. This means that a fully multi-axial hardening needs to be understood and applied. Within the forming process, it can occur that the material is put under tension in both directions after each other, how does the material harden at this point? Every load case need to be covered with a material hardening rule, with load case, compression and tension of the material in different directions is meant. A study related to a more detailed description of material hardening is outside of the scope of this thesis. A study into using kinematic hardening models for multi-axial cyclic plasticity was done by Hancell and Harvey [7]. In this research, kinematic hardening models are used to predict the plastic strain in the material. The study showed that the kinematic hardening model showed a limit to plastic strain while experimental results showed no limit. This means that the mode of deformation could not be predicted by the kinematic hardening model. The kinematic hardening model was used to predict the modes of deformation in a cyclic load experiment. The model also predicts the anisotropy that occurs due to this cyclic loading. The study resulted in the conclusion that the simple kinematic model is not accurately predicting the deformations. The range of elastic unloading that was predicted is not supported by the experiments that were done.

Lin and Hua studied the influence of strain hardening on a continuous roll bending process [17]. They developed a mathematical model to solve differential equations for large deflections including strain hardening. They compared this with perfectly plastic material. A plane strain assumption is made to be able to use beam theory in the mathematical modelling. The conclusion of the research is that strain hardening increases the magnitude of relevant physical quantities concerned for the bending operation. This research suggests that a material hardening rule is necessary in the forming process for double curvature plates. The plane strain assumption that is made needs an further explanation. Strains into the thickness direction of the plate during plate bending are assumed to be zero. This assumption might be used for the three point bending process, but with plate rolling, there is a strain input in thickness direction of the plate, the plate will be thinner after rolling, and this assumption cannot be made. In the previously mentioned study by Rady, the plane strain assumption is made in the rolling direction [23]. Next to plane strain, there is a plane stress assumption. In the plane stress assumption for plates, the stress in thickness direction is assumed to be much smaller than the plane directions. Therefore, the stress in thickness direction is assumed to be zero in the case of a thin plate. These assumptions are both helpful to make a start to a simplified analytical model of the forming processes.

Shakeri studied existing isotropic and kinematic hardening models [28]. The research was done to validate different mathematical models with experiments and compare the results. The conclusion in this paper gives good insight into the possible models that can be used for modeling hardening for specific types of material. A higher strength steel can be modeled with only kinematic hardening characteristics while low yield steel can be accurately modeled with isotropic hardening characteristics.

In the research of Shakeri [28], and an earlier study by Dusicka et al.[5], the Ramberg-Osgood stress-strain hardening relationship is used and proved to be a good model for both higher strength and lower strength steels. The model can be used when specific material parameters are known. This model is used in both studies and concluded to be useful when modeling cyclic strain hardening. The Ramberg-Osgood model[24] is defined in Equation 2.2:

$$\varepsilon = \frac{\sigma}{E} + \left(\frac{\sigma}{K}\right)^N \tag{2.2}$$

where:

K = the strength coefficient in [-]
N = the strain hardening exponent in [-]

In this equation, the first part gives the elastic strain, and the second part is the plastic strain. The K & N parameters are material dependent and can be found when the true stress-strain curve is available.

The Ramberg-Osgood model is not the only stress-strain hardening relationship that can be used. Another law that only describes the plastic part is the Hollomon equation [9], see Equation 2.3.

$$\sigma = K\varepsilon_P^n \tag{2.3}$$

In this equation, only the plastic part of deformation is taken into account. Next to the Hollomon equation, there is a Swift equation [34], see Equation 2.4.

$$\sigma = K(\varepsilon + \varepsilon_0)^n \tag{2.4}$$

Equations 2.2, 2.3 and 2.4 are all using different parameters. The *'N'* parameter in equation 2.2 has typical values in between 1 and 10 with typical values of 5 [6]. The exponent *'n'* in Equations 2.3 and 2.4 has typical values between 0-0.3 [15][16].

To accurately model the forming process, a stress-strain relationship should be used. With all the references in this literature review and most of them using a elastic perfectly plastic material, this will be the main assumption related to material characteristics in analytically modeling the different forming processes. Whenever this assumption gives inaccurate results in future studies related to this topic, one of the discussed equations can be used. To create an analytical model, simplifications should be made, starting with the most simple. The elastic perfectly plastic material assumption, together with plane stress and plane strain assumptions are a start of a simplified model.

In the iterative forming of a double curvature plate, hardening will be important and therefore a hardening law is required in a future study. Remember that the goal is to analytically model the forming process as accurately as possible. With different hardening laws available, a consideration between the applicability and accuracy of the models should be made. This applies to both hardening and the stress-strain relationship. To do this, the research into this topic has to be in a further stage and different questions have to be answered before. A question that arises when thinking about the material hardening and the need of a more realistic stress-strain relationship is what level of plastic strain is expected in the material in each forming operation? The amount of strain per action and the total amount of strain are both important in accurately predicting the material hardening and so the next operations on the same material.

2.6. Research Gap

The main goal of this thesis is to model the forming process of a desired double curved geometry analytically. To do this, a literature review is performed to see what is known about double curvature plates and what is known about the different forming processes of these plates. Next to forming of plates and double curvature plates, there is interesting knowledge related to geometry and mathematics. As a conclusion, the following knowledge gaps were found.

This thesis is focusing on two different forming processes: three point bending and rolling between two rollers. These two processes are all applied on a small part of a large plate. This was the first priority to search for literature. The only study that was found related to local forming process of plate bending was done by Rady [23]. This study focused on the rolling process and is very useful to model the rolling process analytically. The simplifications that are used in this model are well considered, and the steps taken to make the forming model more realistic are well explained. One of the recommendations from this study was the reversed problem, find the controlled rolling method to achieve the desired geometry from a flat plate. This is close to the goal of this study but multiple forming methods are used in this thesis. However, the study by Rady will be helpful to address and analytically model the rolling process.

A local three point bending simulation on a larger plate or on sheet metals was not found. The research by Liu et al.[19] gives an insight in the spring back and residual stresses after three point bending a thick beam. These findings can be used for simplifying the three point bending operation with beam theory. Three point bending over a small fraction of the width of a plate was not found and so this is a knowledge gap.

Research related to spring back, residual stresses and hardening is helpful for accurate description of the material behaviour in the forming process. However, to use these theories and knowledge, the basics of the three point bending and rolling process need to be modeled at first. Therefore, the found research might be helpful after modelling these individual processes.

Another conclusion that can be made is that from previously mentioned research, a lot of forming processes are validated by FEA. This suggests that a validation of an analytical model can be done with FEA. The research with FEA simulations will be helpful to perform a FEA for the particular process [8][11][18][29]. Whenever the analytical model is established, FEA is needed to verify the calculations and the stress and strain distributions in the plate.

The following paragraphs give answers to the asked sub-questions.

The difference between the three point bending and roll compression is the different strain input in the material. Three point bending inserts bending strains while rolling the plate gives membrane strains. Each of these strains result in curvatures in a different way. Local membrane strains give global curvatures and local bending strains give local curvatures.

The deformations and rotation in plates can analytically be modeled by the geometrical mapping research that was found. However, these studies assume that the initial shape of the plate is not known. In this research, it is assumed that the initial flat plate dimensions are optimal for the desired shape. This means that there is not much plate stretching required. Because the initial and desired shapes are known, the deformations and rotation can be calculated by mathematical equations. These findings can then be related to material mechanics by physics. This will be done by simplifying as much as possible. Plate theories will not be used and cross-section of the plate will be simplified as a beam.

The third question is related to a later stadium in this research. The first goal is to describe the forming process of a double curved plate and obtain an accurate result, thereafter optimization of the forming process can be discussed. For now, the accuracy between the formed and desired plate is the key metric to find the forming procedure. In a later study, this process can be optimized by searching for the least amount of bends and shifts of the plate.

There are no other requirements than the used material type and the accuracy of the formed plate. The accuracy of a formed plate needs to be within 5 mm. This accuracy is required by clients of IHC.

The next chapter gives a description of the current practice at IHC, and an example geometry is introduced.

2.7. Methodology

With all the information that is obtained from literature, an approach to answer the research question can be made. This thesis is split into two paths which combination will lead to an answer on the research question. On one side, all information necessary for creating an optimization on the single forming processes is gathered. This means, the difference between initial and desired geometry results in strain fields. Membrane strains as well as bending strains are obtained from these drawings. On the other side, two analytical models that relate the information about the shape to the actual process. The three point bending model has the actual deflections as input. The rolling model has the global curvature and membrane strains as input. After all, a forming procedure can be made for certain cross-sections with the found analytical models and practical experience from the metal workers. The approach is visuzalized in Figure 2.4.

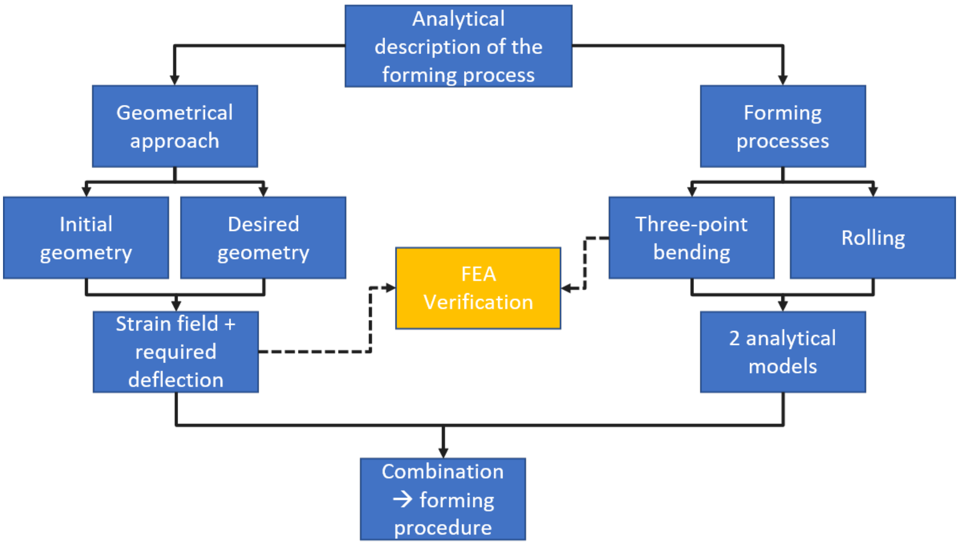

Figure 2.4: Thesis approach

3

Current Practice

Firstly, this chapter describes the information that can be obtained from available data, and an example geometry is introduced. Hereafter, the forming processes and the current practice is discussed. This will lead to a more detailed discussion about the individual forming processes in the next chapters.

3.1. Double Curved Plate

Double curved surfaces can be classified into barrel or saddle shapes. A barrel shaped surface consists of convex curves over both axes. A saddle shaped surface consists of a concave over one axis and a convex over the other axis. Figure 3.1 shows the visual differences between a barrel and a saddle shaped surface. Both these shapes can also be found in Figure 1.1. The barrel shaped plates are found in the bulbous bow, while the saddle shaped plates are found in the transition from the bow to the side hull. These kind of shapes are also found in the stern of a vessel.

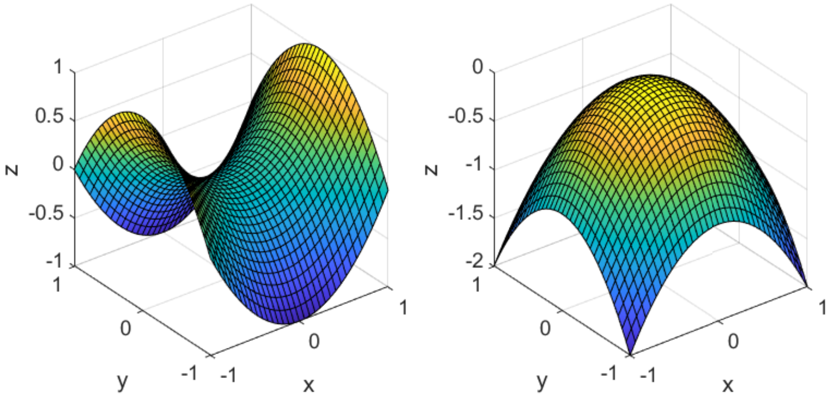

Figure 3.1: A saddle and barrel shaped surface respectively

The example geometry is a saddle shaped plate, see figure 3.3. The plate has a thickness of 12 mm. The maximum length and width are respectively, 4464 mm and 401 mm. The yield stress of the material that is used is 305MPa. Both, the initial and desired shape, are found in Figures 3.2 and 3.3 respectively. These drawings can give information about the desired plastic strains to form the initial into the desired shape. The 3D-coordinates are fit with a surface equation of fourth order polynomial form. The fit has an accuracy of 99.7 %. The equation that is obtained can be found in equation 3.1.

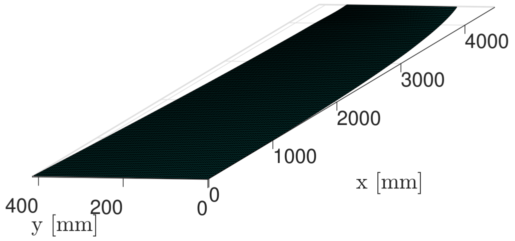

Figure 3.2: The initial flat plate before forming

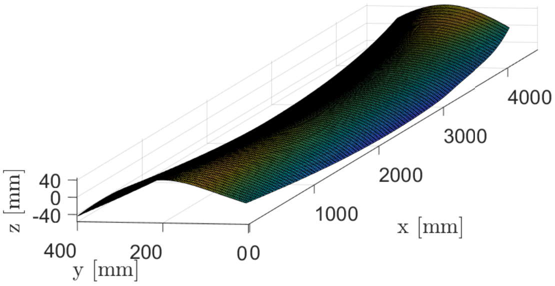

Figure 3.3: The desired shape of the plate

$$\begin{aligned} Z(x,y) &= 1.63\cdot10^{-13}\,x^4 + 7.52\cdot10^{-12}\,x^3\,y + 1.35\cdot10^{-9}\,x^3 \\ &+ 1.20\cdot10^{-11}\,x^2\,y^2 - 1.32\cdot10^{-10}\,x^2\,y - 8.21\cdot10^{-7}\,x^2 \\ &+ 3.73\cdot10^{-10}\,x\,y^3 + 1.66\cdot10^{-7}\,x\,y^2 - 2.85\cdot10^{-5}\,x\,y - 0.031\,x \\ &+ 1.61\cdot10^{-9}\,y^4 + 6.62\cdot10^{-7}\,y^3 - 0.0019\,y^2 - 0.820\,y - 46.84 \end{aligned} \tag{3.1}$$

where:

x = the length coordinate in [mm]
y = the width coordinate in [mm]

3.1.1. Membrane strains

The surface equation can be used to calculate lengths for a certain cross-section following equation 3.2. Comparing the lengths of the desired shape with the lengths of the initial shape, the amount of membrane strain can be found. A positive membrane strain suggests material stretching, while a negative membrane strain suggests material shrinkage.

$$L = \int_a^b \sqrt{1+\left(\frac{dz}{dx}\right)^2}\,dx \tag{3.2}$$

$$\epsilon = \frac{L-L_0}{L_0} \tag{3.3}$$

where:

a, b = start and end coordinate in [mm]
L = the length of a line-piece of the desired shape in [mm]
L_0 = the length of a line-piece of the initial shape in [mm]

The length is calculated for a certain cross-section, so for a particular y-coordinate in this case. This can be done for a cross-section over the other axis as well. The amount of membrane strain in the length direction and width direction can be found in Figures 3.4 and 3.5. By using the conservation of volume, see Equation 3.4, the amount of thinning can be calculated to acquire the desired membrane strains. In the conservation of volume, as well as in the rolling model in chapter 5, a plane strain assumption is made. This means that the strain into the width or length all come out of rolling in that certain direction. For example, $\epsilon_y = 0.02$ in Figure 3.5. This means that the absolute thickness reduction over the total width for the example geometry will be 0.24 mm.

$$\epsilon_1 + \epsilon_2 + \epsilon_3 = 0 \tag{3.4}$$

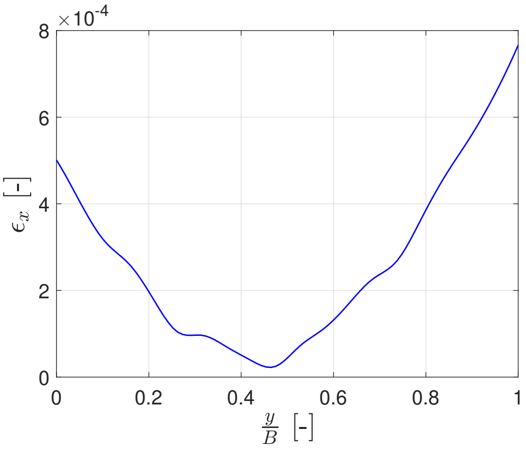

Figure 3.4: The total membrane strain over the length of the plate at a certain y position

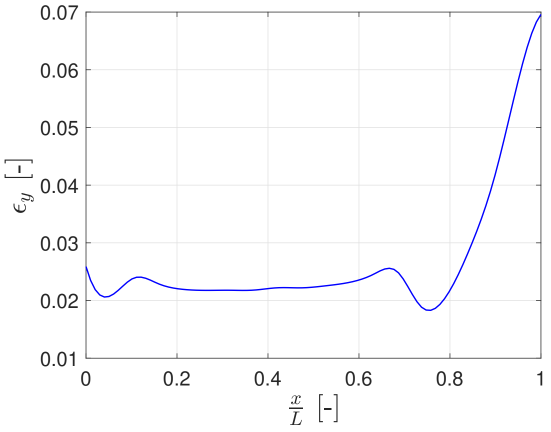

Figure 3.5: The total membrane strain over the width of the plate at a certain y position

The membrane strain will be discussed in more detail in Chapter 5.

3.1.2. Bending Strains

Next to membrane strains, the surface equation can give information about the curvatures. Mathematical curvatures of a plane curve can be calculated following equation 3.5. The curvatures are directly related to bending strains following equation 3.6. For each cross-section of the plate/surface, x or y is constant, the curvatures can be calculated.

$$\kappa = \frac{\left|y''(x)\right|}{\left[1 + (y'(x))^2\right]^{\frac{3}{2}}} \tag{3.5}$$

$$\epsilon = \frac{h}{2}\kappa \tag{3.6}$$

where:

h = the thickness of the plate in [mm]
κ = the curvature in [1/mm]
ϵ = the bending strain in [-]

The desired plastic membrane and bending strains, which can be calculated with equations 3.3 and 3.6, give information for the two forming processes. Next to the deflection and coordinates, the membrane and bending strains will be used as input for the forming processes. With this information, a prediction of the forming process can be made. In the following section, a brief introduction into the two forming processes is given. The characteristics of the two forming machines that are used are given.

3.2. Forming Processes

The double curved plate is formed by bending and rolling. Three point bending introduces bending strains, while rolling mainly introduces membrane strains. Both rolling and bending are local processes, which means that a plate is never rolled or bent over its entire length or width at once. This is confirmed by the dimensions of both machines, see Figures 3.6 and 3.7.

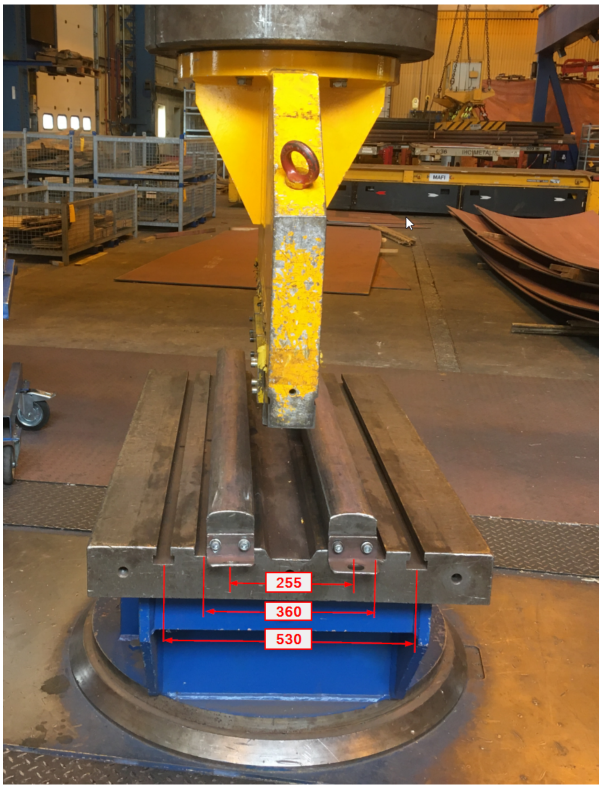

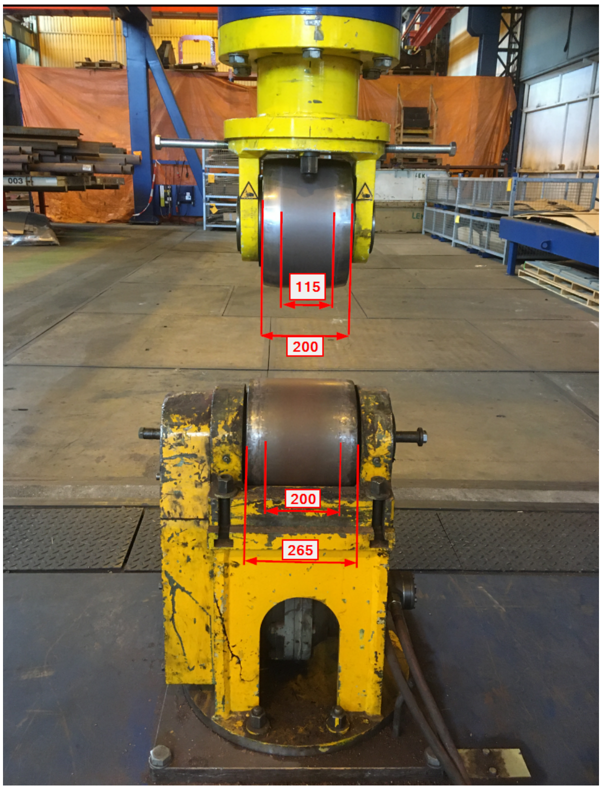

Figure 3.6: Three point bending machine at IHC, dimensions are in millimeter [1]

Figure 3.7: Rolling machine at IHC, dimensions are in millimeter [1]

These machines can form a flat plate into a double curved plate. The maximum rolling and bending force are 500 and 100 tonnes, respectively. In practice, these forces are never used, and the force is slowly increased during multiple repetitions at a single location. As mentioned, this thesis focuses on a saddle shaped plate. The saddle shaped plate is formed by first introducing curvatures over the width axis at first. Where after the length axis curvature is initiated by rolling the edges of the length axis. This process is captured in a video by Nieland, the fabricator of these machines [21]. The operator needs approximately 20 presses over the width of the plate for the bending process. For rolling, the operator needs approximately ten passes over one edge to initiate the second curvature. The operator checks the shape with wooden moulds in between the passes. If there is no gap between the mould and plate, the plate has the correct shape. For a barrel shape, the operator rolls the center of the plate instead of the edges. In this way the second curvature is initiated over the center line which results in a barrel shape.

4

Three Point Bending

In this chapter, the three point bending operation is analyzed. This operation is visualized in Figure 4.1, which is simplified with beam theory. Beam theory focuses on 2D beams, while in reality, a plate is bent locally resulting in 3D effects. Another simplification that is introduced in this chapter, is the use of an elastic-perfectly plastic material. Also, material hardening is not taken into account.

In the next Section 4.1, a single bend of a beam with the three point bending machine is investigated analytically. This bend is verified by FEA in Section 4.2. With equations of the deflection, an optimization into beam bending is done in Section 4.3. The optimization will result in the minimum amount of bends to achieve the desired shape.

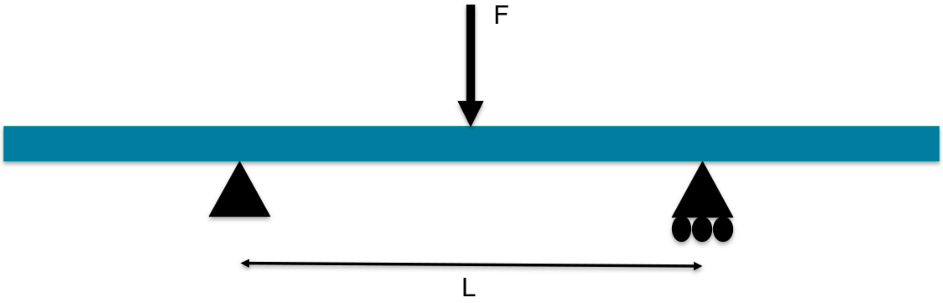

Figure 4.1: Three point bending of a beam with rectangular cross-section

4.1. Single Bend

The analytical three point bending operation is visualized in Figure 4.1. The moment distribution for the three-point bending beam is shown in Figure 4.2. The beam is supported at locations A and C, and it is loaded at point B. From point A to be D, the deformation is all elastic. From point D to E, it is mixed elastic and plastic, with the plastic part increasing as it gets closer to E. From E through the thickness, the beam can be considered as fully plastic, meaning that the elastic portion in the center is negligible. This thesis focuses on plastic deformations. Because the plates are being deformed plastically, well-known elastic beam equations cannot be used. A study by Štok and Halilovič [32] is used to describe the deflection of rectangular beams in the elasto-plastic phase. The elasto-plastic phase is visualized in Figure 4.2. The elasto-plastic phase is defined by the internal moment laying between the full plastic moment and the elastic moment. As mentioned before, this is in between point D and E. In this phase, plastic strains arise, and permanent deformation is present after unloading. In the study by Štok and Halilovič [32], a solution for the deflection is found. The equations are related to the moment distribution of the beam. In this three point bending case, the moment distribution is linearly increasing up until the middle of the beam as shown in Figure 4.2.

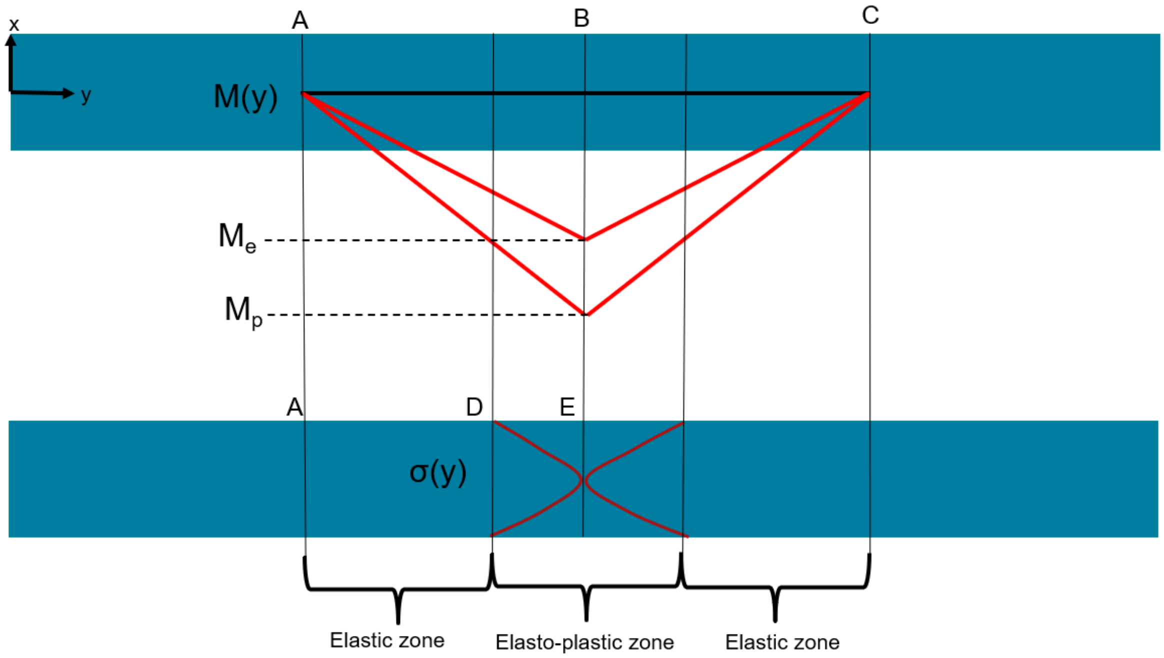

Figure 4.2: Moment distribution and stress distribution over the thickness for a full plastic hinge

The deflection can be calculated up until a full plastic hinge. A plastic hinge concludes that the yield stress is reached over the entire thickness of the beam, induced by a full plastic internal moment. The moment that is applied is equal to this fully plastic internal moment per unit width, M_p in Figure 4.2. The corresponding deflection is given in Figure 4.3. The deflection is calculated by Equations 4.1 and 4.2. Equation 4.1 describes the deflection up until the yield moment, while Equation 4.2 the deflection in the elasto-plastic phase describes. This means that with a full plastic moment that will be applied, Equation 4.1 is valid up until $\frac{2}{3}L$, and Equation 4.2 is valid after that up until L.

$$\delta(x) = \frac{\frac{4M_p}{L}x}{48EI}\left(3L^2 - 4x^2\right) \tag{4.1}$$

where:

I = the moment of inertia in [mm^4]
x = the length position on the beam in [mm]

The deflection for the elasto-plastic phase can be calculated with the following equation:

$$\delta(x) = \frac{4K}{3m_1^2}\sqrt{\left(M_p - \|M(x)\|\right)^3} + \delta_H \tag{4.2}$$

where:

$$K = \operatorname{sign}(-M(x))\sqrt{\frac{b\sigma_{yield}^3}{3E^2}}$$
$$m_1 = \frac{-M_p}{L/2}$$
$M(x)$ = the moment function in [N · mm]
δ_H = the homogeneous solution to establish continuity

The corresponding deflection curve can be found in Figure 4.3.

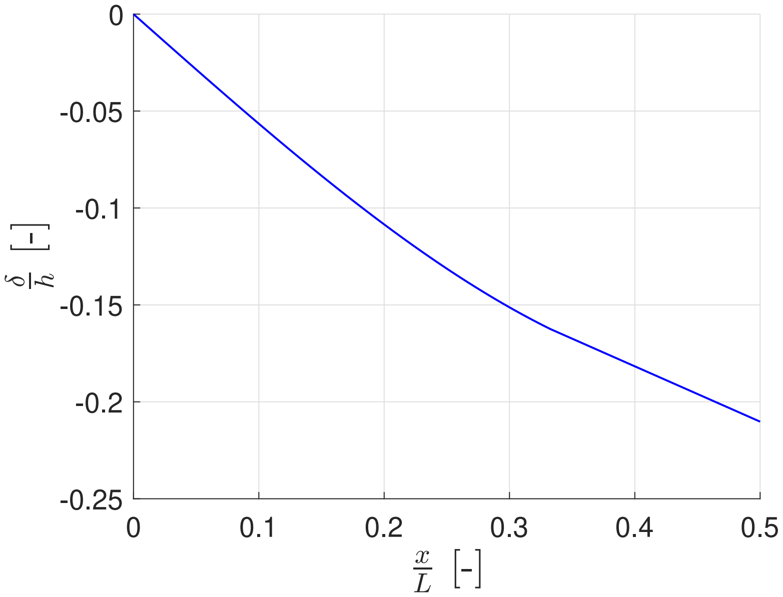

Figure 4.3: The deflection for a full plastic hinge with constant distance between supports

To calculate the force required for initiating a plastic hinge, equation 4.3 is used. This equation gives the force per unit width. This is calculated from the global equilibrium.

$$F_{external} = \frac{4M_p}{L} \tag{4.3}$$

Where:

L = the distance between the supports [mm]
M_p = the plastic moment per unit width [N·mm/mm]

4.1.1. Support Distance

As mentioned, the three point bending operation is simplified as in Figure 4.1. The actual bending operation is visualized in Figure 4.4. This simplification needs some attention related to the press and the supports. During a single bending operation, the contact area of the press increases. Also, the contact location of the supports changes. These phenomena affect the analytical calculations for the deflection and required force. A decrease of the support distance increases the force that is needed for a full plastic hinge. In the this section, an analytical approach to take into account the change of the support distance is given. Thereafter, FEA is used to verify the deflection, the force and the support distance during the bending operation.

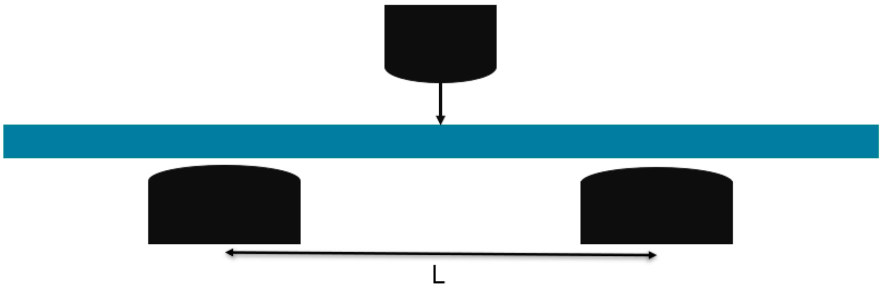

Figure 4.4: Actual bending operation supports and press

For an accurate calculation of the required force for a certain deflection, the decreasing distance between the supports should be taken into account. The function that calculates the distance between the supports is based on the geometry change during the deflection. Figure 4.5 visualizes the distance between the press and a support. Because of symmetry, only one half is visualized. On the basis of this figure, a solution approach is found for the decreasing distance between the supports.

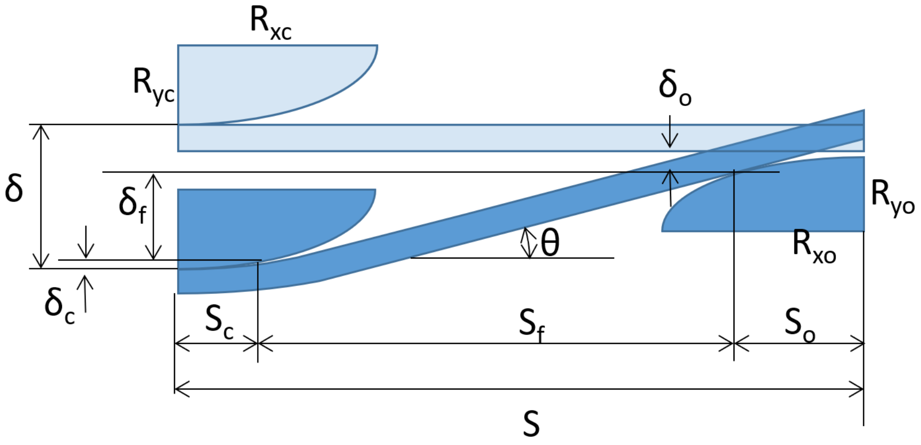

Figure 4.5: Contact locations of the press and support

The varying parameter in finding the distance between the press and support (S_f) is the deflection (δ). If the deflection is known, the distance between the press and support is known and the force required to achieve the deflection can be calculated. The relation between the deflection and support distance is found by following the next steps:

1. Assume θ
2. Solve equation 4.4 for S_c and S_o
3. Calculate δ_c and δ_o by equation 4.5
4. S_f and δ_f can be calculated by the total δ and S

$$\tan(\theta) = \frac{R_{yc}}{R_{xc}^2} \cdot S_c \sqrt{1 - \frac{S_c^2}{R_{xc}^2}} \tag{4.4}$$

$$\delta_c = R_{yc} - R_{yc}\sqrt{1 - \frac{S_c^2}{R_{xc}^2}} \tag{4.5}$$

Where:

δ_c, δ_o = the height of the contact location between the beam and press or support [mm]
δ = total deflection of the beam [mm]
θ = the angle of the beam between the press and support [rad]
R_{xc}, R_{xo} = half the length of the press and support [mm]
R_{yc}, R_{yo} = the height of the press and support [mm]
S_c, S_o = contact length of the press and support [mm]
S = total distance between the press and support [mm]

Now that all the parameters given in Figure 4.5 are known, a range of angles θ are substituted and the system can be solved for every θ. This results in a deflection over the distance between the supports plot. This is visualized in Figure 4.6.

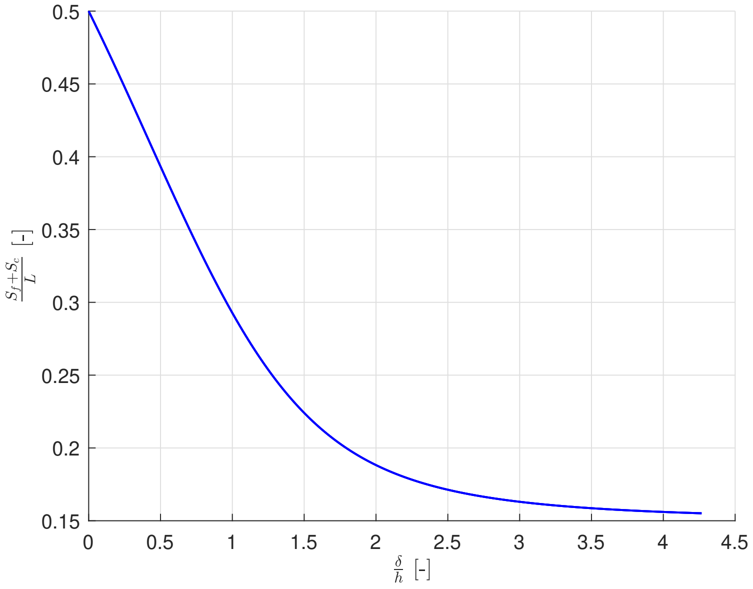

Figure 4.6: The normalized deflection is plotted over the normalized distance between the two supports

In this figure, the support distance is defined as the distance between the center of the press and the contact location of the support ($S_f + S_c$). This distance is needed for the calculation of the actual required force, following equation 4.3, the total distance between supports is needed. The actual distance between the supports will be twice the distance that is given in this figure. This distance will be calculated by using this figure as a look-up table.

At this point, a relation between the deflection and support distance is found. This relation is verified in Chapter 4.2. After the verification of the support distance and deflection, the related external force can be calculated. Before the external force can be calculated, an internal plastic bending moment is needed. To calculate the plastic bending moment, the yield stress in y-direction of the beam is needed. The solution for finding the yield stress in y-direction is given in the next subsection 4.1.2.

4.1.2. Von Mises Criterion

To calculate the force required for a plastic hinge and the yielding moment, the Von Mises yield criterion has to be rewritten. This needs to be done because a 2D instead of a 3D problem is investigated. To calculate the yield stress in y-direction, Hencky's equation is used [36], see equation 4.6. Hencky's equation is used instead of Hooke's law, because plastic strains are the interest of this research. In Equation 4.6, ϵ_3 is assumed to be zero. Together with the assumption that $\sigma_1 = 0$, this leads to an unique relationship between σ_1 and σ_2. The Von Mises yield criterion in Equation 4.7 can be rewritten, see Equation 4.8, and the yield stress in y-direction becomes 352 MPa. This yield stress is used to calculate the plastic moment and external force with equations 4.9 and 4.3, respectively.

$$\epsilon_3 = \frac{1}{E_s}[\sigma_3 - \frac{1}{2}(\sigma_1 + \sigma_2)] \tag{4.6}$$

Where:

σ_1, σ_2,and σ_3 = principal stresses in [MPa]
E_s = secant modulus in [MPa]
ϵ_3 = third principal strain [-]

$$\sigma_\text{v} = \sqrt{\frac{1}{2}\left[(\sigma_1 - \sigma_2)^2 + (\sigma_2 - \sigma_3)^2 + (\sigma_3 - \sigma_1)^2\right]} \tag{4.7}$$

$$\sigma_{\mathrm{v}} = \sqrt{\frac{1}{2}\left[\sigma_2^2 + \left(\frac{1}{2}\sigma_2\right)^2 + \left(\frac{1}{2}\sigma_2\right)^2\right]} \tag{4.8}$$

With the calculated yield stress, the plastic bending moment per unit width can be calculated, see equation 4.9.

$$M_p = \frac{1}{4}h^2\sigma_2 \tag{4.9}$$

In the next section, the deflection and external force are verified by FEA.

4.2. FEA verification

FEA is used to verify the force and related deflection of the beam. FEA is also used to capture the spring back after a single bending operation. The geometry used for the analysis can be found in Figure 4.7. During the analysis, the decreasing distance between the supports is monitored as well. At first, the distance between the supports is monitored until a fully plastic hinge is achieved resulting in verification of Figure 4.3. Hereafter, the analytical force can be calculated based on the distance between the supports.

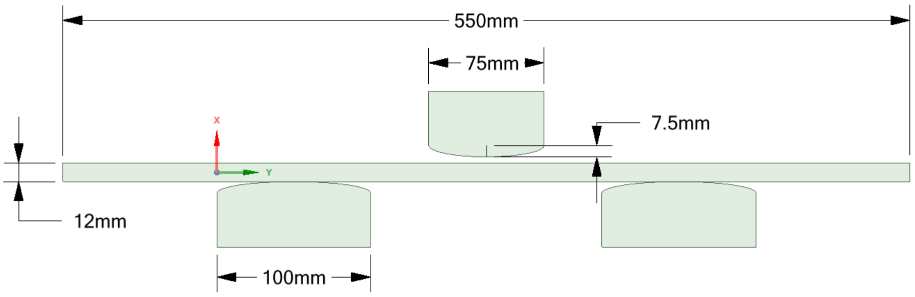

Figure 4.7: The geometry used in FEA

The 2D FEA is performed to capture the stress in y-direction, following the coordinate system in Figure 4.7. The 2D FEA is assuming plane strain. This means, zero strain in z-direction. To capture the stress over the thickness of the beam, 12 elements are created over the thickness. The mesh can be found in Figure 4.8. The supports and the press are defined as structural steels with the yield stress being equal to 1000 times the yield stress of the beam. This is done to assume the supports and press as rigid bodies. Finally, the contact between the supports, press and beam are modeled as frictionless.

Then, a simulation is performed with a large displacement. During this simulation, the distance between supports is captured up until a full plastic hinge develops. The analytical external force is calculated with a constant distance between the supports (L = 250 mm). This is done to find a first estimate of the force required for a full plastic hinge. In the first simulation, the exact moment where a full plastic hinge is formed is close to the calculated external force. Hereafter, the simulation is repeated up until the found plastic hinge in the first simulation to investigate the spring back and support distance change. In the next section, the plastic hinge is visualized and compared to the analytical plastic hinge.

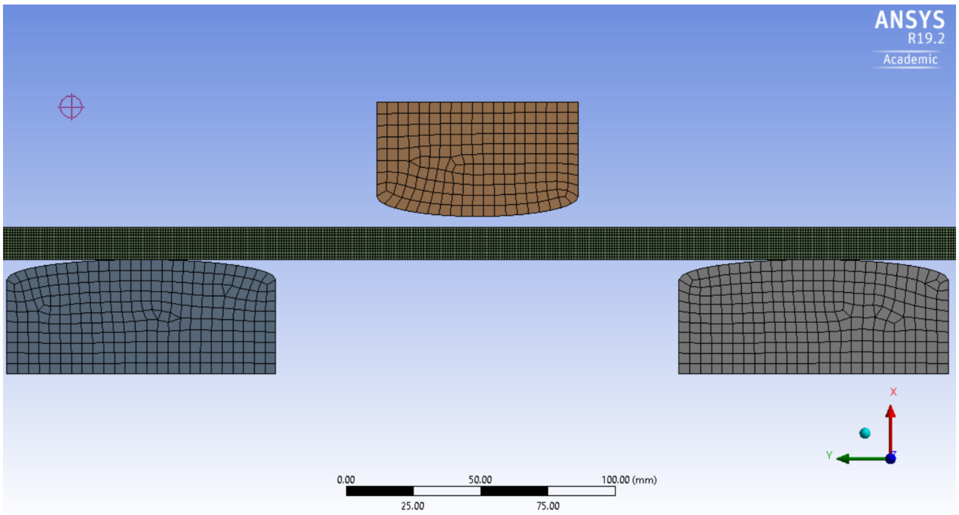

Figure 4.8: The mesh size in the FEA simulation

4.2.1. Plastic Hinge

The analytical through thickness stress distribution for a fully plastic hinge can be found in Figure 4.9. The FEA will not give the same stress distribution. The reason for this is that there cannot be a discontinuity in the stress distribution through thickness. Next to that, the contact of the press with the beam will cause higher compressive stresses than expected by the analytical calculation. In Figure 4.10, the stress distribution of the simulation is given at 2.5 mm deflection of the beam. The visualization of this stress distribution in ANSYS is given in Figure 4.15.

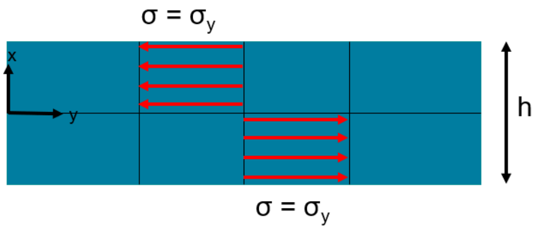

Figure 4.9: Through thickness normal stress for a full plastic hinge

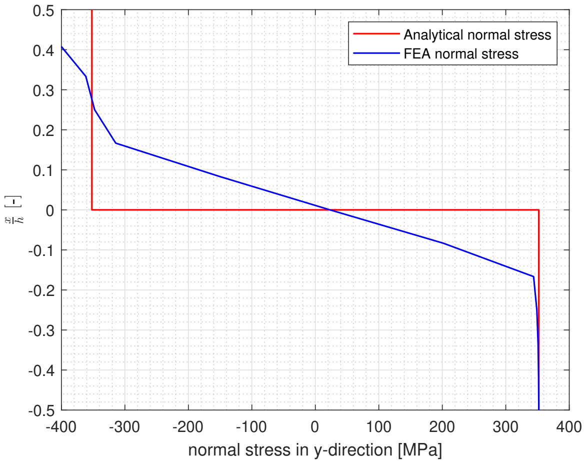

Figure 4.10: Through thickness normal stress obtained from the FEA

The analytical force for a plastic hinge is calculated for a constant distance between the supports. The analytical force for the yielding moment is also calculated. The relation between the yielding moment and the plastic moment is the shape factor of the cross-section. A rectangular cross-section, such as the plate, has a shape factor of 1.5. This results in the following relation, see equation 4.10.

$$M_e = \frac{2}{3} M_p \tag{4.10}$$

Where:

M_e = yielding moment in per unit width [N·mm/mm]

In Table 4.1, the analytical force for the yielding and plastic moment are given. In Section 4.2.3, these forces are recalculated based on the actual support distance and compared to the numerical forces.

Table 4.1: Analytical forces for yielding and plastic moment calculated

Support Distance [mm]	Analytical Force for M_p [N/mm]	Analytical Force for M_e [N/mm]
250	202.8	135.2

4.2.2. Support Distance

Now that the analytical force for a constant support distance is calculated, the support distance change over time needs to be verified. With the support distance change over time, a more accurate estimate can be made for the force related to a plastic hinge. The goal is to verify Figure 4.3. In the simulation, a deflection of half the thickness is applied. The focus is on the first linear part of Figure 4.3. The support distance is obtained at multiple time steps during the applied deflection. Next to that, a difference is made between the longest and shortest distance between the supports. This difference is visualized in Figure 4.11. In this figure, the contact locations are mentioned as sliding in the legend. The simulation is not taking friction into account because this is also not done for the analytical equations, so sliding can be seen as contact. In the end, the analytical and numerical results are compared in Figure 4.12.

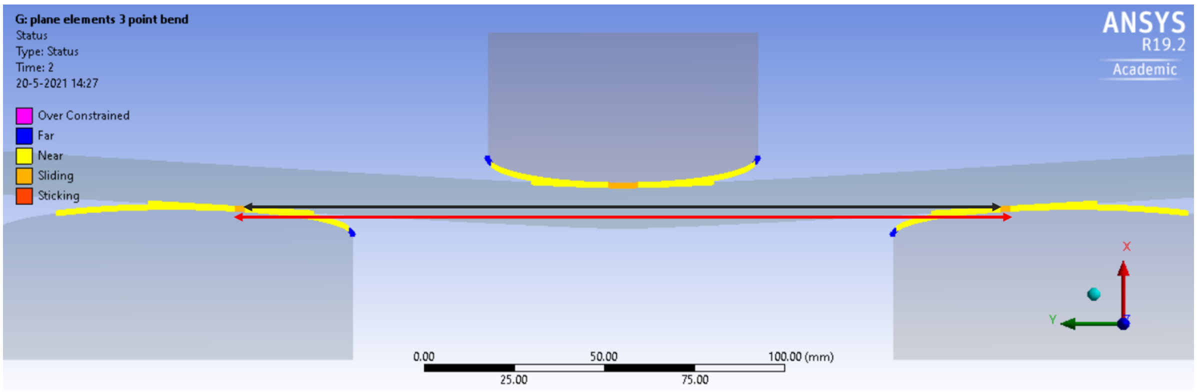

Figure 4.11: Difference between long and short distance of contact in ANSYS. Red is the longer and black is the shorter distance.

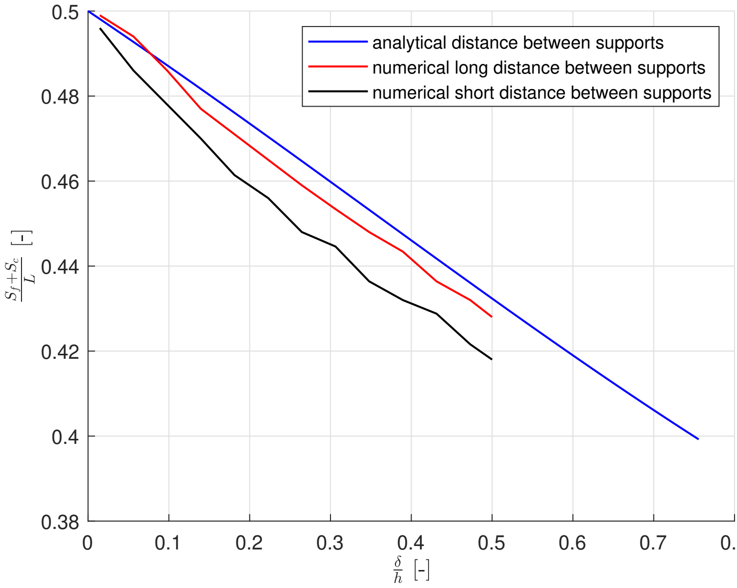

Figure 4.12: Comparison of analytical and numerical distance between the supports

The difference between the analytical and numerical support distance is explainable by the fact that the analytical equation does not take into account the thickness of the beam. Nevertheless, the long distance between the supports is close to the analytical result, and therefore, this support distance can be used to calculate the external force required for a certain deflection.

4.2.3. Analytical Force

The analytical force corresponding to first yield and a fully plastic bending moment for a constant support distance is calculated and can be found in Table 4.1. Now that the support distance relation with the deflection is established, the actual analytical forces can be calculated and compared with FEA. Before that, the deflection needs to be verified. The deflection plot for a support distance of $L = 250$ mm is given in Figure 4.3. This is the deflection under loading. In the end, this thesis focuses on the plastic deformations and therefore the deflection after unloading. Both the deflection under loading and after spring back are obtained from the simulation. The spring back is equal to the elastic deflection. This is visualized in Figure 4.13. Both the under loading and after spring back deflections do agree. The differences are explainable by the fact that the analytical deflection calculation does not take into account the increase of the contact area of the press.

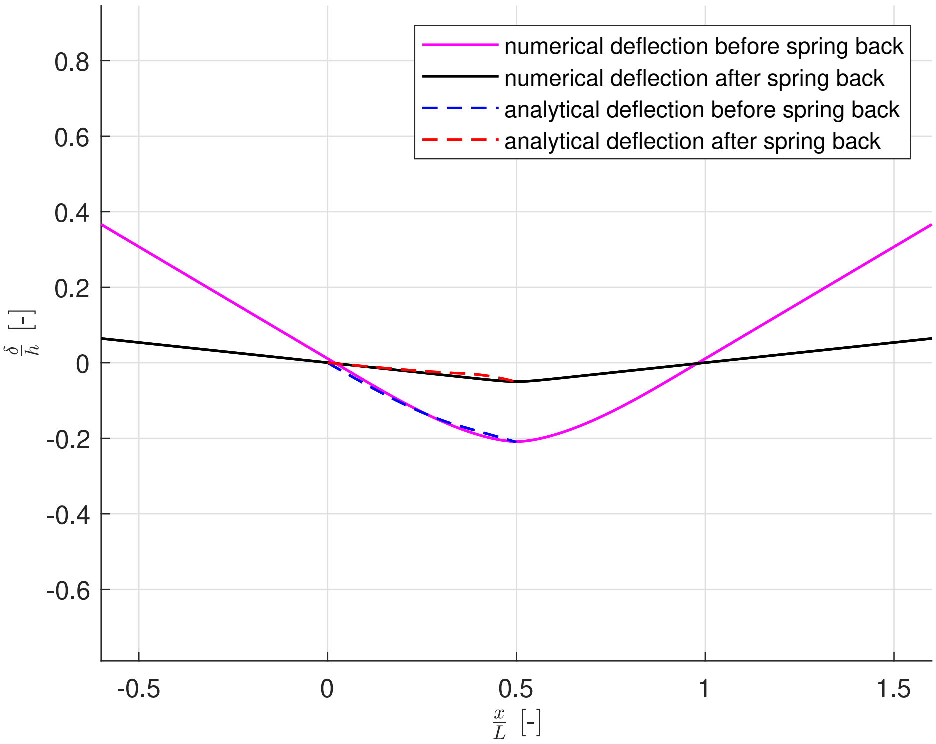

Figure 4.13: The analytical and numerical deflection before and after spring back

The analytical deflection is only plotted for a single half and in between the supports. Something that stands out is that the numerical deflection under loading does not cross $\frac{x}{L} = 0$. The reason for this is the decreasing distance between the two supports during loading. However, after springing back, the deflection of the simulation in ANSYS intersects with $\frac{x}{L} = 0$. The angle also agrees with the analytical calculation. The only difference in the deflection is related to the simplified three point bending, and that the increasing contact area is not taken into account.

The deflection is verified, the next and final step is to look into the external forces required for a full plastic hinge. As explained, the deflection related to a plastic hinge can be found in Figure 4.3. This deflection is calculated for a constant support distance. In Figure 4.13 it is shown that this deflection fits the numerical deflection. The support distance related to this deflection is looked up on the blue line in Figure 4.12. In Table 4.2, the analytical support distance and related external force are compared to the numerical results. The external force is calculated by equation 4.3 with L as the actual support distance. This means the support distance related to the amount of deflection is used to calculate the external force. This is done for the yielding moment and for the plastic moment.

Table 4.2: Comparison of the analytical and numerical results

	Yielding Moment	**Plastic Moment**
Analytical deflection over thickness [-]	0.127	0.210
Analytical support distance over maximum distance [-]	0.966	0.944
Analytical external force [N/mm]	140	215
Numerical deflection over thickness [-]	0.116	0.208
Numerical support distance over maximum distance [-]	0.969	0.936
Numerical reaction force [N/mm]	149	220

The yielding moment is visualized in Figure 4.14. The plastic hinge is visualized in Figure 4.15.

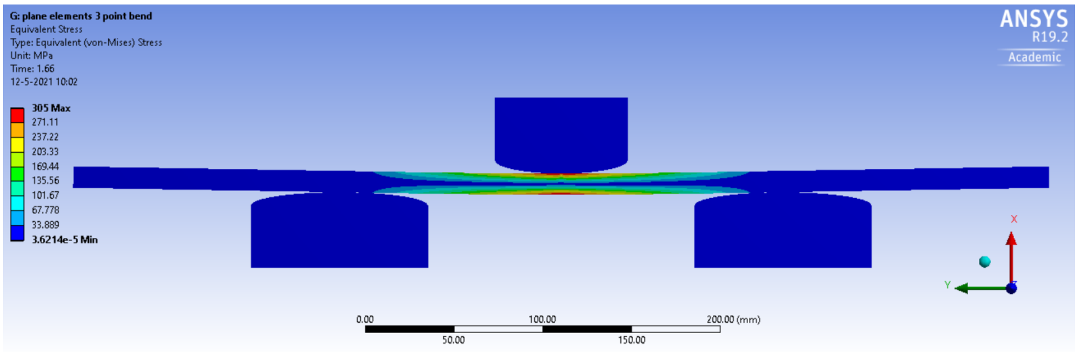

Figure 4.14: First material yielding during the bending simulation

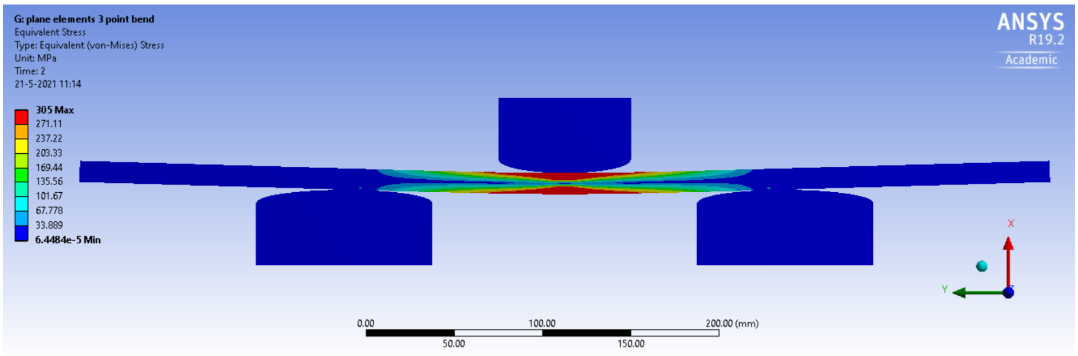

Figure 4.15: Full plastic hinge that arises during bending operation

4.2.4. Conclusion

The goal of the single bend verification is to find realistic analytical equations for the deflection. Next to that, the deflection needs to be related to the external force of the machine. The external force is the input for the machine and the metal worker. The external force that is calculated for a plastic hinge is 2.5% lower than the force obtained by FEA. This is a reasonable difference and related to the fact that the analytical bending operation is more simplified than the FEA simulation.

Therefore, the main improvement of the deflection and force calculation can be found in a more realistic approach of the analytical equations. The increase of the contact area should be taken into account over time or over the amount of deflection. For now, the obtained results can be used for the bending optimization in the next section.

4.3. Bending Optimization

On site experience shows that three point bending is the first step in creating a saddle shaped plate. The plate is then rolled in specific areas to initiate a second curve. An optimization is performed to find the least number of bends necessary to form a flat beam into a desired curve. The optimization is simplified to 2D beams. In reality, 3D effects are present and an optimization of a cross-section, which can be seen as a beam, does have an impact on the starting shape of the neighbouring cross-section. Next to the 3D effects, the optimization does not take material hardening or existing residual stresses into account. The optimization starts with a flat beam, and finds the locations and amount of deflection necessary to achieve the desired shape. The optimization minimizes the difference between the actual and desired shape which optimally results in the least number of bends. The optimization uses the single bend deflection that was introduced in Chapter 4.1. It is assumed that this is the maximum deflection that can be achieved in a single bend. A larger deflection can be achieved in reality; however, the equations that are used for finding the deflection of a plastic hinge are limited to the maximum plastic moment.

4.3.1. Setup

As mentioned previously, the optimization searches for the least amounts of bends necessary to form the flat beam to the desired shape. A requirement for the forming process is the accuracy of the formed beam. The maximum allowable difference in shape is 5 mm. So, the optimization is focusing on an accuracy of 5 mm with the least amount of bends. At first, the cross-sectional data is rewritten and an initial direction of the flat plate is set. The cross-section at the end of the plate (X = L) is investigated in this section as an example. Both the initial direction of the beam and desired shape are given in Figure 4.16. The absolute values of the length and deflection are used in this optimization to give a better insight in what happens during the optimization.

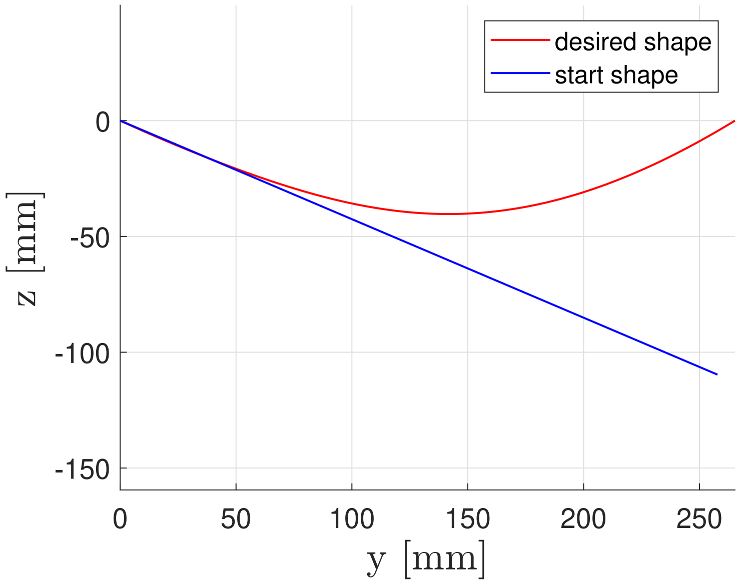

Figure 4.16: Desired and initial cross-section at $x = L$

An important note to Figure 4.16 is that the length of the initial shape is equal to the length of the desired shape. Previously, it was mentioned that the width of the plate needs a significant amount of membrane strain. For this bending optimization it is assumed that no stretching is required, and that the length during the bending optimization is constant.

4.3.2. Optimization Procedure

The optimization focuses on the smallest difference between the desired and start shape. In the optimization, there is sought for a location to bend from left to right. The reason behind this is that the metal worker does not have to move the plate from left to right and back. The first step is to find a location to bend. Whenever the mentioned distance is larger than 5 mm, a first location to bend is found. The second step in the optimization process is to check if a bend can be added at the found location. The bending operation is constraint by the distance between the two supports (250mm). The length of the start shape in the example is equal to 280 mm. This means that there is just a little space for the beam to move. A new location to bend is suggested whenever the first found location is impossible to bend because of the beam not laying on the supports. The suggested location is equal to half the distance between the supports plus another 10 mm margin.

After finding the location for the first bend, a deflection equal to the deflection of a single plastic bend is added. Hereafter, the distance between the desired and initial shape is checked. If the distance is found to be within 5 mm accuracy, a next location to bend is sought for. If this is not the case, another bend will be performed at this location.

The optimization stops whenever the beam is not supported by the support on the right side, or whenever the actual shape is within 5 mm of the desired shape at every location.

4.3.3. Results

For the example geometry this optimization is performed multiple times with different setups. At first, the 250 mm support distance is used. This resulted in one single location to bend, the amount of deflection at this location is equal to 16 times a single bend. As known, the deflection did not match the FEA deflection perfectly. Therefore, the kink that can be found in Figure 4.17 will not be found in reality. In Figure 4.17, the final result on this optimization is given.

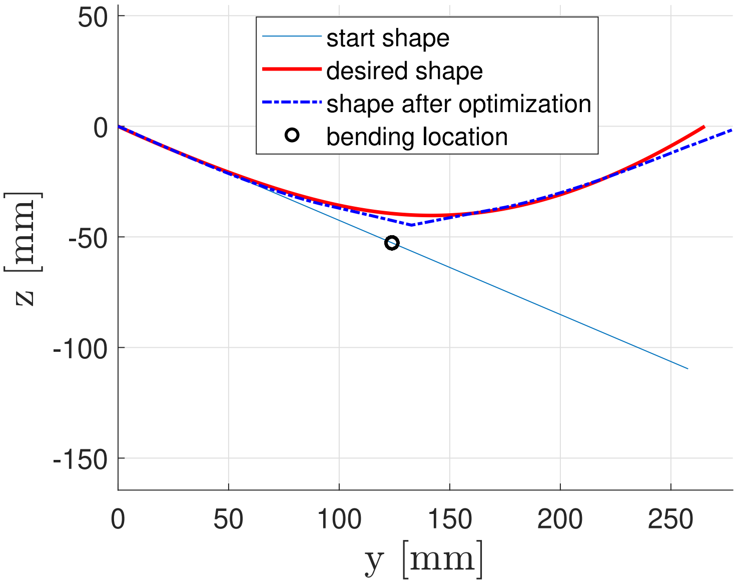

Figure 4.17: Result of the first optimization from the example geometry

It can be concluded that this is not the exact shape that is desired. Especially not at the right half. No curvature can be added at this half because there is no support for the plate. Therefore, the optimization is performed again with a shorter support distance, 100 mm. This way, the range to apply bends is much larger, and more bends can be added over the beam. Another reason for this, is that the used example is definitely smaller than an average shipbuilding plate. By using a shorter support distance, the ratio between the support distance and width of the plate comes closer to larger plates. The result of the optimization with 100 mm support distance is visualized in Figure 4.18.

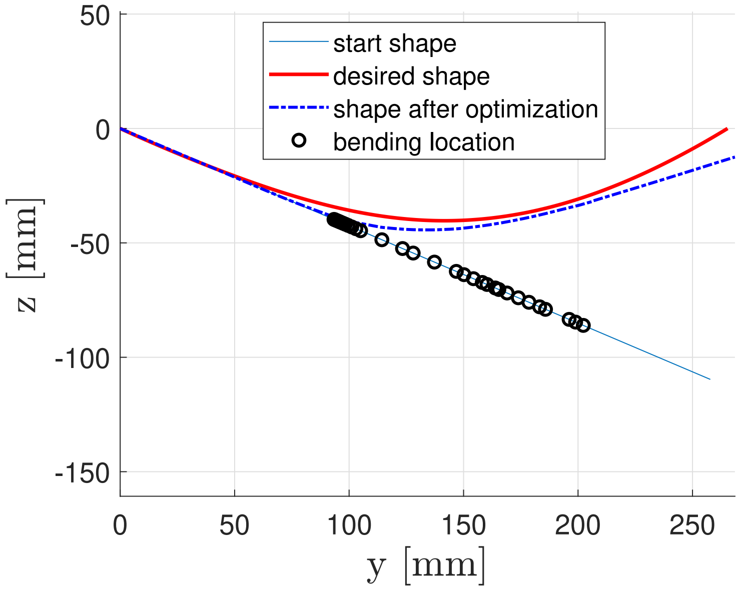

Figure 4.18: Result of the same optimization with 100 mm support distance

One last optimization is performed for a support distance of 75mm. With this setup, approximately 75% of the beam is in range to bend. This is equal to a plate of one meter with the original support distance. The result of the optimization with 75 mm support distance is visualized in Figure 4.19.

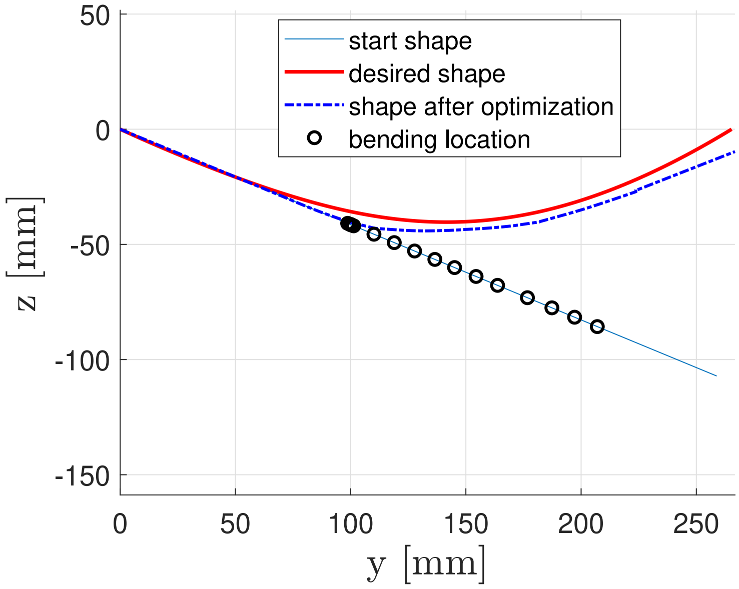

Figure 4.19: Result of the same optimization with 75 mm support distance

The amount of bends at all the locations is given in Table 4.3. The difference between different support distances is given. One important note to these results is that the maximum deflection of a single bend is constraint by the deflection related to a plastic hinge. With a shorter support distance, a plastic hinge is found with a smaller deflection. This makes it hard to compare those results. The increased range makes bending at the edges of the plate possible which definitely results in more accurate curvatures and results.

Table 4.3: Optimization results for different setups

Support distance [mm]	250	100	75
Total number of bends [-]	16	61	56
Total number of bending locations [-]	1	30	9
Maximum number of bends at single location [-]	16	7	21
Maximum deflection of single bend [mm]	0.61	0.10	0.055

The optimization process can be improved by looking into different functions to minimize. At this point, only a single local coordinate is minimized by adding a deflection. The deflection at this single location effects the shape of the overall beam. Therefore, a combination between the local difference and the overall difference might result in a better shape.

After all, it can be concluded that the smaller support distance results in better control of the shape near the beam ends. For a plate with a maximum width of approximately 400 mm, the support distance of 250 mm is relatively large, which makes it harder to control the shape. Whenever the overall process is taken in mind, the machine operator does not want to change the setup for the machine at different cross-sections. Also, during bending different plates, changing the setup costs time. However, it is recommended to use a smaller support distance for the example geometry. It can be assumed that the example geometry has a larger length over width ratio than average which makes it hard to draw good conclusions.

4.4. Practical Relevance

Finding the bending procedure for an initially flat cross-section helps the machine operator to know where and with what force to bend. In the example geometry, the operator knows to bend the plate in the center multiple times. In reality, the operator might apply a larger force at once to give the plate more deflection in a single operation. However, the location and total amount of deflection, and related bending operations and forces are known. For a larger ratio between the support distance and cross-section size, a forming procedure that leads to a more accurate result can be found. This is helpful for the machine operator because a larger range to bend the cross-section is present. For now it is assumed that every cross-section starts with a initial flat shape. Whenever 3D-effects are known, a cross-section that is affected by bending at another place can be used into the model. This leads to less bending operations. In a future study, this can be solved, and an accurate description of the bending locations on the full plate can be given. This way, the operator exactly knows the bending locations to create the U-shaped plate before the rolling process. In the next chapter, the rolling process is investigated. The rolling force distribution over a cross-section over the length will be given to initiate the second curvature.

5

Plate Rolling

One of the two processes to form a flat plate into a double curved plate is plate rolling. A picture of the plate rolling machine can be found in Figure 3.7. As mentioned, the rolling process focuses on rolling the plate in lines that are 115mm wide. This chapter focuses on equations that relate the required membrane strain, of the rolling lines, to the rolling force. Next to that, the membrane strain is related to the global curvature of a plate. In Chapter 3, a description of the membrane strain is given. The required membrane strain per cross-section is also given. The membrane strain is directly related to plate thinning because of conservation of volume in plastic deformation. In reality, the rolled path is restricted to stretch by the material on the sides of the rolling path. This will lead to a curvature over the rolling line. This gives an idea about the global equilibrium that can be made of the plate. But first, the analytical rolling model to relate membrane strains to a rolling force will be discussed. A study by Salimi and Sassani is used to calculate the rolling force [27]. In this study, the general case of asymmetrical plane strain rolling is described with a slab method. The analytical model in this study is validated by available experimental data. Therefore, the model is valid to use for the specific rolling case used by IHC. The analytical model is rewritten such that the input is the required membrane strain at specific locations, and the output is the required rolling force per unit width. This rolling model will be discussed in more detail in the next section. Thereafter, local membrane strains are related to the global curvature.

5.1. Rolling model

As mentioned, the analytical rolling model is established from the study by Salimi and Sassani [27]. The model is based on the cross-section in Figure 5.1. This model is using the plane strain assumption. This means that thickness reduction results in membrane strain into the rolling direction. Multiple asymmetrical parameters are highlighted in Figure 5.1. Some of the dimensions of the rolling machine used by IHC are given in Figure 3.7. Next to these, the roller diameter of both rollers is 300 mm. Another assumption is that the friction coefficients of both rollers are equal. The only asymmetrical aspect in the investigated rolling machine is that only the bottom roller is mechanically driven. Due to no difference in friction coefficients and an equal diameter of both rollers, the ratio between the rotational velocity of both rollers is assumed to be 1.

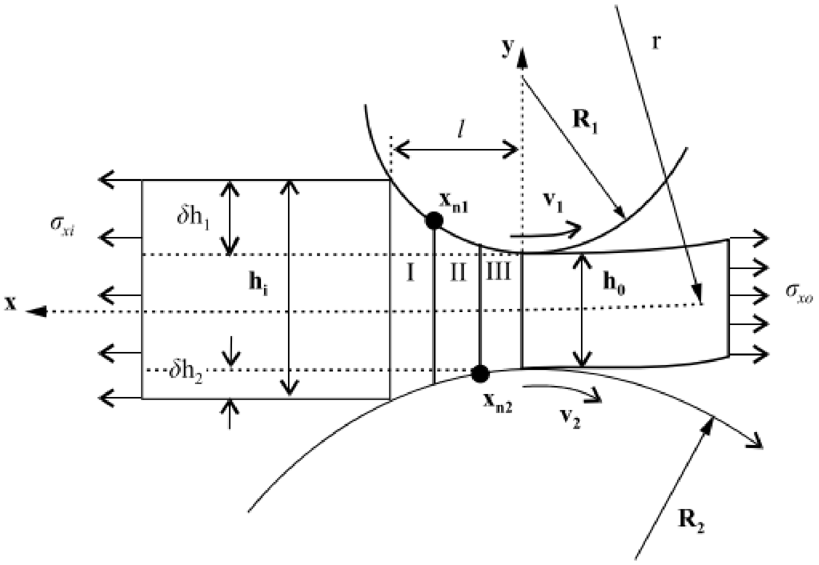

Figure 5.1: The assumed geometry based on the study by Salimi and Sassani [27]

In this figure, three different zones are mentioned (I, II and III). The rolling pressure distribution can be calculated for every zone. This leads to the calculation of a rolling force. The three zones represent the shear stress directions. In zone one and three, the shear stress direction is the same at the top and bottom. The shear stress in zone one is opposed to the shear stress in zone three. Due to asymmetry in the process, a second zone arises. In this zone, the shear stress direction at the bottom and top are opposed to each other. This is an important reason for a curvature that arises during the roll process. As mentioned, the investigated process is assumed to be symmetrical. Therefore, the second zone is not present. In another study by Tian et al, the rolling pressure distribution for a representative case is presented [35]. This case is used to check if the used analytical model gives the same results. This verification is performed by using the values as suggested in a specific case without any asymmetry. This resulted in the same rolling force per unit width. After checking the programmed model, the analytical model is rewritten so that the input is the membrane strain and the output is the rolling force per unit width. The rolling force per unit width is then multiplied by the width of the upper roller to find the actual required force for a certain membrane strain.

5.1.1. Rolling Force

As can be seen in Figure 3.4, the membrane strain over the width decreases by a factor three from the edge to the center of the plate. Also, the width of the roller is equal to 115 mm while the plate is just 400 mm wide. This means that approximately 3.5 rolling lines can be created over the width of the plate. The highest required plastic strain is equal to $6.9 \cdot 10^{-4}$ mm/mm. This is just 45% of the yield strain from Equation 5.1.

$$\epsilon_{yield} = \frac{\sigma_{yield}}{E} \tag{5.1}$$

Where:

σ_{yield} = the yielding stress in [MPa]
E = the Young's modulus in [MPa]

However, the amount of deflection over the full length of the plate is also small, approximately 40 mm deflection over a length of 4000 mm. To achieve the required plastic strain, spring back has to be taken into account for the rolling process as well. This means that the strain initiated under rolling needs to be equal to the plastic strain plus the elastic strain. The elastic strain is calculated by Equation 5.1. Equation 5.1 only gives the elastic strain in the perfectly plastic condition as assumed in this research. Whenever a hardening material is used, the elastic strain increases with increased plastic strain. By assuming perfectly plastic material, the plastic strain that remains after spring back is equal to the desired plastic strain.

The largest required strain results in a rolling force of 11.6 tonnes. This is 2% of what the machine can apply. Initiating the second curvature is not only related on the required membrane strain in length direction. A global equilibrium of the plate together with the rolling model can give a better insight in initiating a second curvature. A possible approach for finding the required deflections and membrane strains by using a global equilibrium will be discussed in the next section.

5.1.2. Global Equilibrium

The rolling forces and paths can be found by using global equilibrium. The global equilibrium relates local membrane strains to the global curvature. As mentioned before, the amount of deflection over a single cross-section over the full length is relatively small, approximately 1 %. The discussed cross-section can be found in Figure 5.2. The actual length and thickness of this cross-section are 4468 mm, and 12 mm, respectively. In this figure, a polynomial fit is made through the coordinates. The polynomial equation is used to calculate the curvature over the cross-section.

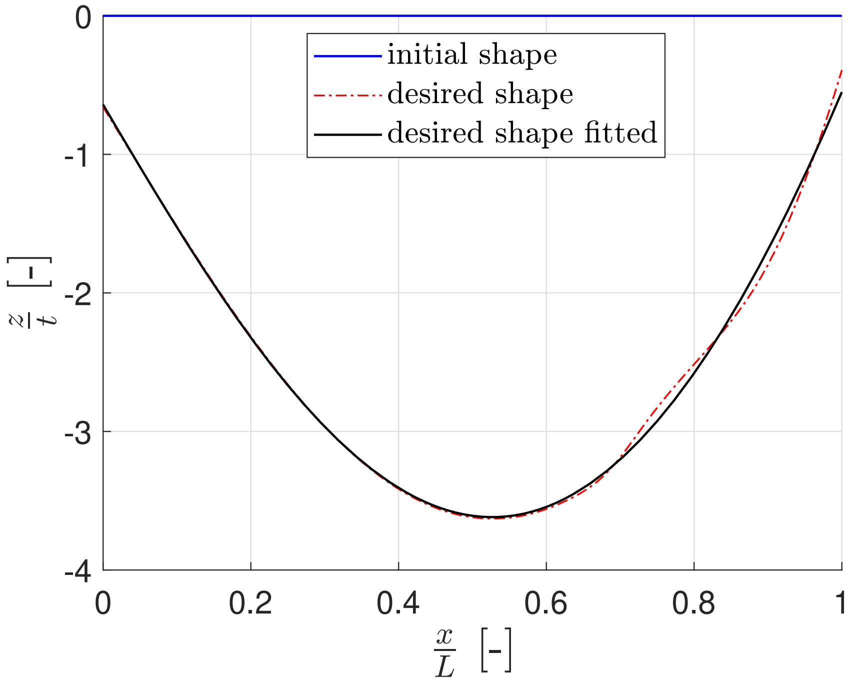

Figure 5.2: Initial and desired cross-section of one edge of the example geometry, y/B = 0

In this figure:

L = length of the plate in [mm]
t = thickness of the plate in [mm]
x = length coordinate of the plate in [mm]
z = deflection of the plate in [mm]

Figure 5.3 visualizes the top view of a rolling line. The scale of the figure is approximately the same as of the machine and the example geometry.

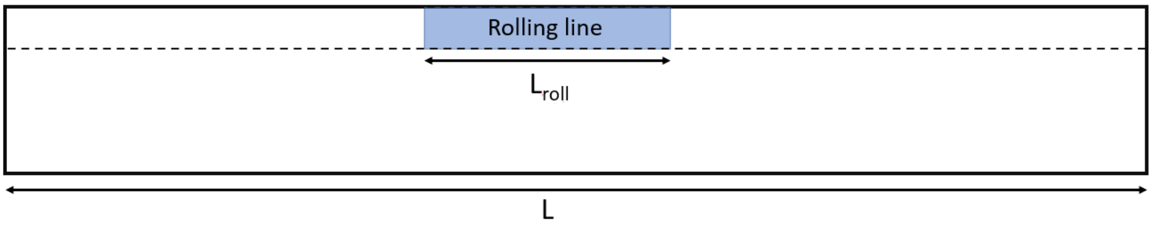

Figure 5.3: Top view of a possible rolling line

The relationship between local membrane strains and global curvature defines the global equilibrium. The relationship between these two arises by looking into the rolling process, required membrane strains and required curvature. As mentioned previously, the rolling process is assumed to be in plane strain. This means that thickness reduction results in strain into the rolling direction, and the strain perpendicular to the rolling direction can be assumed to be zero. Research by Shin et al. confirms this assumption [31]. The used plate and roller dimensions in the study by Shin et al. are smaller. However, it is not expected that this is of significant influence on the strain perpendicular to the rolling direction. In Figure 3.4, it was concluded that the highest required membrane strain is equal to $6.9 \cdot 10^{-4}$ mm/mm. This is the required strain over the total length of the cross-section. The required strain does not directly mean that every part of the rolling line needs to be rolled with constant force resulting in an evenly distributed strain over the given cross-section.

The curvature over the particular cross-section is given in Figure 5.4.

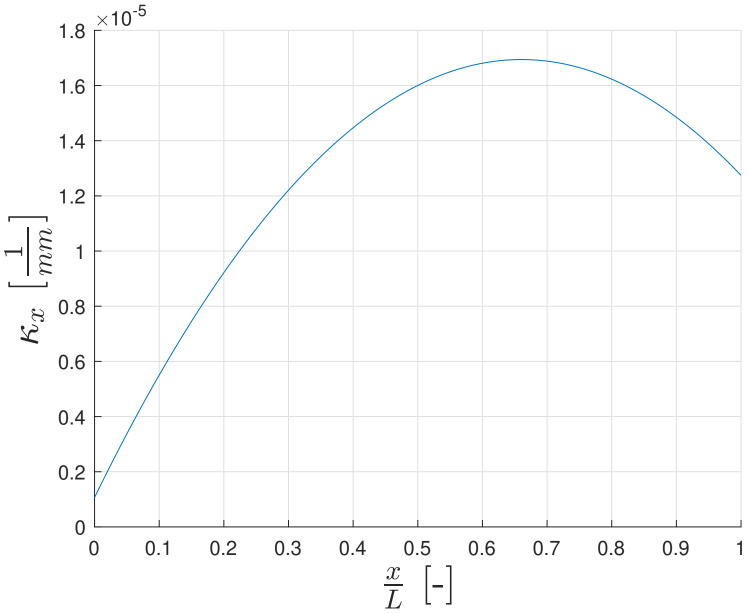

Figure 5.4: Curvature over the same cross-section as in Figure 5.2, y/B = 0

The curvature distribution is calculated by applying Equation 3.5 to the polynomial equation of the cross-section. This leads to the curvature over the cross-section. Based on this curvature distribution, the membrane strain over a certain length can be calculated. In calculating the membrane strain over a fraction of the length of the cross-section, it is assumed that the length increase results in deflection. This assumption is made to find a relation between the local membrane strain and the global curvature. The simply supports are used because the material of the rest of the plate restricts the plate from stretching at this point. This is visualized in Figure 5.5.

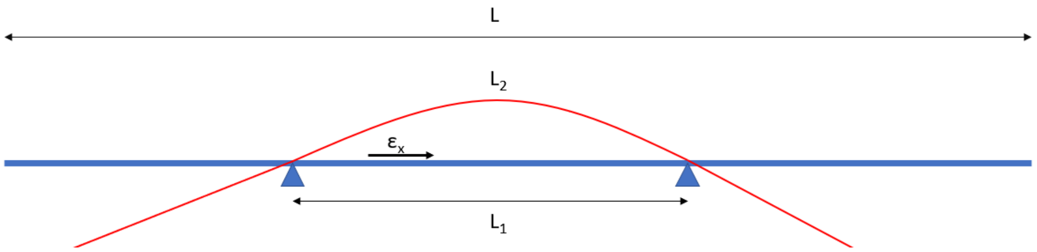

Figure 5.5: Deflection for a part of the plate due to rolling

In this figure, L_1 is the length of a part of a cross-section, ϵ_x is the membrane strain in this part of the cross-section.

The cross-section in Figure 5.2 is split in 10 different pieces. To calculate the deflection of every part, the average curvature of this part is captured. This average curvature is assumed to be constant over the line piece. This assumption leads to calculating the arc length. Figure 5.6 gives the overview of a certain part.

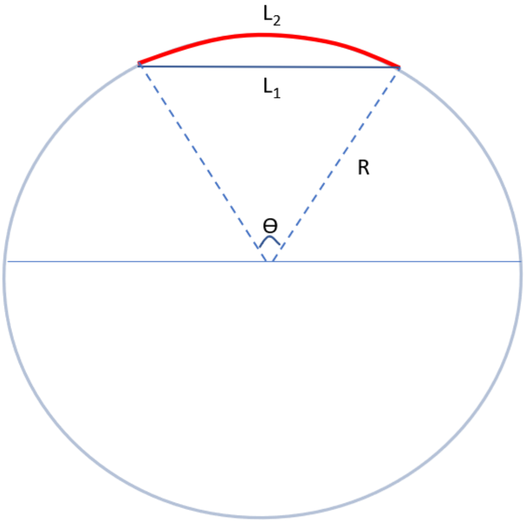

Figure 5.6: Overview of line part

Based on the length of the initial part (L_1) and the radius of curvature, the length of L_2 can be calculated following Equations 5.2.

$$\begin{aligned} L_2 &= \theta R \\ \theta &= 2\arcsin\left(\frac{L_1}{2R}\right) \end{aligned} \tag{5.2}$$

The figure gives a large part of the circle as piece of the total cross-section. The visualized scale in this figure is not the reality. In reality, the ratio between the arc length that is used and the radius of curvature is much larger. The part of the circle that is used for this order of curvatures is about 0.01%. This is calculated by comparing θ in Equation 5.2 with 2π, the full circle.

With the arc length and the initial length, the membrane strain of this part can be calculated following Equation 3.3. This way the membrane strain for every part can be calculated, this is the relation between the curvature and the local membrane strain. Now for every part, this particular part of a circle is calculated. These parts need to be connected into a continuous line. This line will then fit the same shape as the desired shape in Figure 5.2. To connect each part, the minimum in Figure 5.2 is used as top of the circle. This means that where the minimum of the deflection is found, the x-location is put as the origin. Then the cross-section is divided in ten pieces and an arc is calculated for every part. These arcs are connected which finally results in the shape in Figure 5.7. The desired shape as is also plotted again.

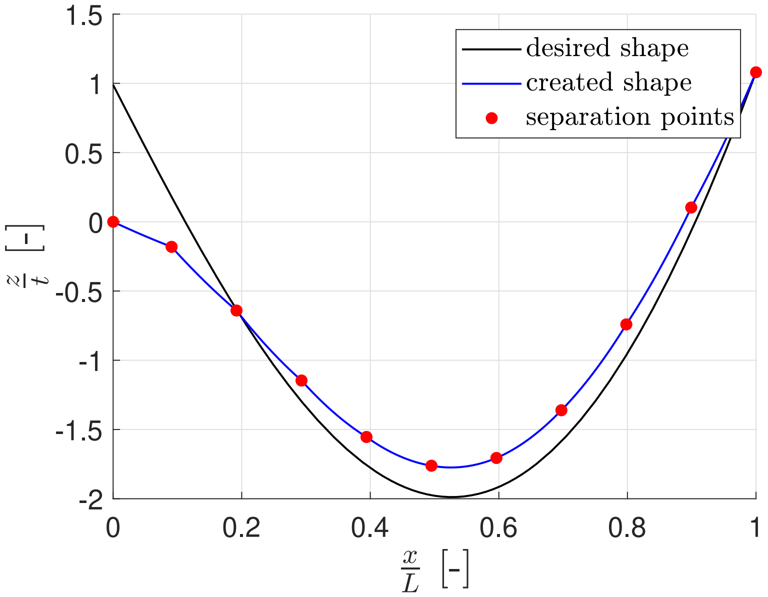

Figure 5.7: The created shape and desired shape at y/B = 0

The difference between the desired and created shape at the start of the plate can be related to the abrupt increase of the radius of curvature. The radius of curvature of each line part matches the radius of curvature of the desired shape. A mistake is present in the visualization. The connection between each part should be continuous. Due to the significant change in radius of curvature, this discontinuity is clearly visible at the left side. In reality, there will not be such a discontinuity.

To create this shape, it is assumed that the membrane strain in a certain part is all transformed into deflection. The plastic membrane strains required to achieve these deflections are given in Figure 5.8. This figure has the same shape as the curvature plot in Figure 5.4 except for one point. The reason for this differing point is the way the membrane strain is calculated. The membrane strain is calculated based on the length of the arcs in 5.6 and the absolute difference in x-coordinates of the initial shape. This means that if there is a certain change in the y-direction of the initial shape, this is not taken into account. The discussed cross-section is the cross-section for y = 0 mm in Figures 3.2 and 3.3. In here can be seen that there is a curvature into y-direction of the initial plate.

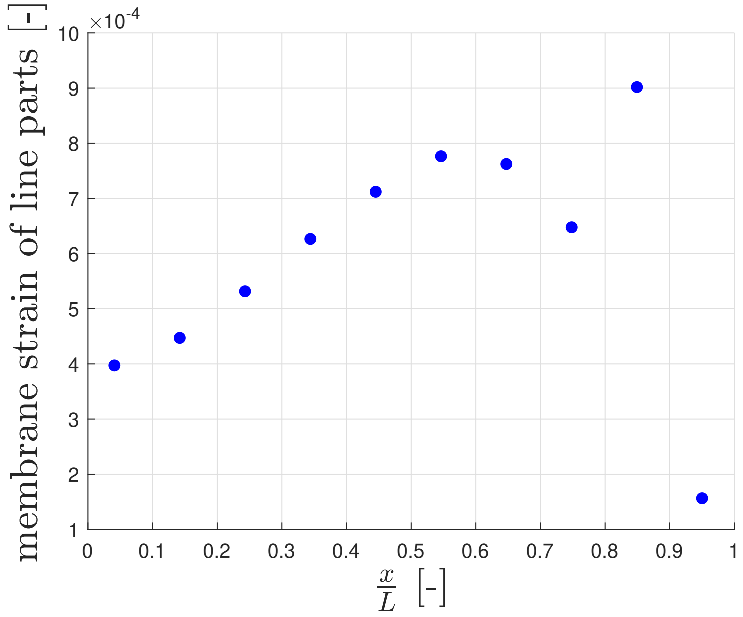

Figure 5.8: Required membrane strain for desired curvature at y/B = 0

The total membrane strain of this cross-section was previously calculated based on the geometry. Now that the membrane strain is also calculated based on the global equilibrium, a comparison is given in Figure 5.9. What stands out in this figure is the negative membrane strains in the middle of the plate. These negative strains are explainable by the fact that the membrane strains are calculated based on a discretized curvature distribution. Next to that, the values for curvatures are really small in the center of the plate. This results in errors in the discretization.

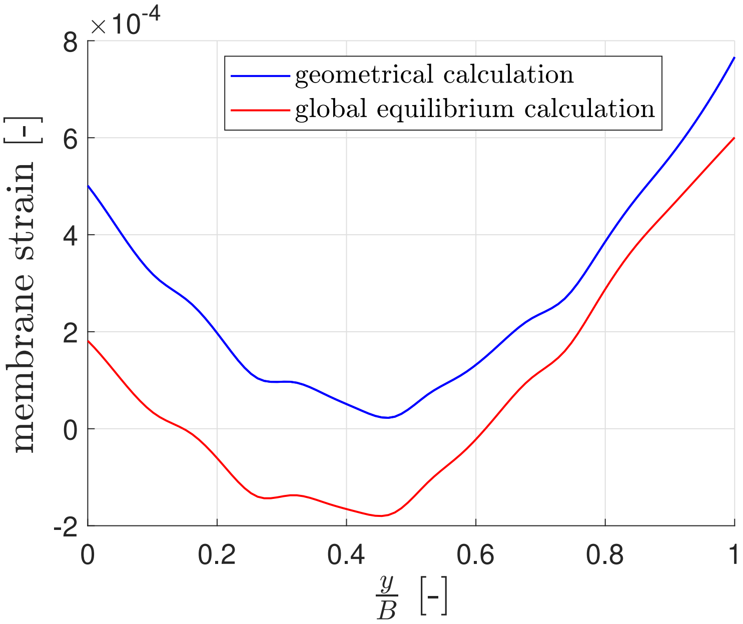

Figure 5.9: Membrane strain geometrical approach and global equilibrium approach

Practise gave the insight in how a saddle shaped plate will be formed. Therefore, the negative strains obtained by the global equilibrium approach can be ignored. To create a saddle shaped plate only the edges will be rolled. The maximum membrane strain of 0.0008 in Figure 5.8, requires a rolling force of approximately 11.5 tonnes. This force is required at the edge to create a curvature over this cross-section. For a barrel shaped plate, the membrane strain in Figure 5.9 will have the opposite shape. In this case, the middle of the plate should increase in length to obtain a barrel shape. To conclude, in general, a U-shaped plate is obtained by the bending operations. This U-shaped plate is then rolled over the edges to stretch the plate and initiate the desired curvature over these edges. While the middle (y/B = 0.5) of the plate keeps the same length.

5.2. Practical Relevance

The relation between the membrane strains, curvatures and rolling forces gives insight in the forming process for the machine operator. Even a look into a simplified 2D-cross-section gives an insight in the required forces and rolling lines. As shown in Figure 5.9, the saddle shaped plate is created by stretching the edges of the plate. For every cross-section the total membrane strain is known, as well as the distribution of the membrane strain over this cross-section. From practise it was already known that the edges should be rolled to create a saddle shaped plate. This thesis confirmed that knowledge, and added the required force distribution over the edges based on the curvature of this cross-section. At least, it is known that the maximum force over the edge is 11.5 tonnes for the example geometry. The video by Nieland [21] learned that rolling multiple passes over a edge are required. This indicates that the total required force of 11.5 tonnes at a certain point is not applied at once. In practise this path will be rolled multiple times with a smaller force. The amount of repetitions is not exactly known. The distribution of the membrane strain gives information about which part of the cross-section should be rolled more times or with higher forces.

5.3. Conclusion

In this chapter, a working and verified model is found to relate membrane strains to the rolling force. Next to that, a method to relate the global curvature to a membrane strain is given. The method requires some fine tuning in visualizing the actual found shape. To confirm this method, more research is required into plate rolling. In general, a relation between membrane strains and curvature is found. As well as a relation between membrane strains and rolling force. A verified model for the relation between membrane strains and forces is found. The relation between the curvature and membrane strains is not verified or validated.

6

Conclusion and Discussion

In this chapter, the general conclusions of this thesis are given. The research question will be answered, and finally several results are discussed.

6.1. Conclusion

The goal of this thesis was to analytically describe the forming process that is required to form a flat plate into a desired double curvature shape. The forming process consists of two different forming machines, rolling and bending. The following research question was formulated after the literature study:

How can the forming process by rolling and bending of a double curved steel shipbuilding plate be analytically modeled?

The forming process is analytically modeled by relating the geometrical information obtained from the drawings to the characteristics of the two forming processes. An analytical description of the forming process can give machine operators a better understanding of the behaviour of the plate during the process. Next to that, a procedure for the forming of a particular shaped plate can be given which helps to give the craftsmen an idea of where to bend and roll the plate. Ultimately, in a future research, this process can be optimized into a more time efficient process.

The general conclusions that can be drawn in this research are related to the information that can be obtained by the drawings, the three point bending process, and the rolling process. At first, information is obtained by the drawings of the initial and desired geometry. Bending and membrane strains are calculated using these drawings. These strains, combined with the actual deflection, are used as input for the forming processes. The three point bending process is modeled using elasto-plastic beam theory. This model creates local curvatures and deflections on the cross-section. These local curvatures and deflections result in the desired global shape. The deformation, spring back and external force of the three point bending operation are verified by FEA. The model is used to optimize the forming process for a cross-section of the plate. The optimization resulted in a procedure to form a beam into the desired shape. This procedure gives the location and amounts of bending operations at these locations to form the plate.

Hereafter, an existing rolling model was used to relate membrane strains to a rolling force. The transverse plane strain assumption is also used for this rolling process as it was suggested in the existing model. The rolling model is not verified by FEA because the existing model was verified for a similar symmetrical process. Next to the relation between the force and membrane strains, a relation between the curvature of the plate and the membrane strains was found. This relation is established by assuming that a membrane strain input of a certain line part results in deflection. Stretching of a certain rolling path results in deflection because the material outside of the rolling path is not stretched. This results in a length difference between two cross-sections and this can only result in a curvature over the rolled path. The curvature is varying over the cross-section. This leads to a varying required amount of membrane strain and so a varying rolling force over the rolling path. Instead of varying the force over a rolled path, some parts of the path will be rolled multiple times with a constant force to achieve the required amount of membrane strain. The relation between the curvature and membrane strains is not verified by FEA.

Concluding, the forming process is analytically modeled by separating the processes. Every process can relate strains to a machine input force. The processes are used to describe the cross-sections over both axes. The rolling process focuses on the longer axis, and relates membrane strains to curvatures over the full cross-section. The bending process focuses on the shorter axis, and focuses on the actual deflection to create a forming procedure of a certain cross-section. Both processes are related to cross-sections, and 3D-effects are not taken into account. For a cross-section over the width the forming procedure for the bending process can be given to give the machine operator a insight in the material behaviour and how to achieve the desired shape. This also applies for the rolling process. The force distribution over a cross-section over the length axis results in the desired curvature over this cross-section. This also gives insight for the machine operator.

6.2. Discussion and Recommendations

A lot of assumptions and simplifications are used in this thesis. This brings up a discussion at some points. This section describes these discussion points, starting with general assumptions. At first, both the rolling model, and three point bending model focused on beam theory. This means that 3D-effects that occur in reality are not taken into account. With 3D-effects, the behaviour of the rest of the plate, if one cross-section is rolled or bent, is meant. In this study, it is assumed that only the investigated cross-section is affected. This should be the main focus in a future study. The challenge in this, is finding 3D-analytical equations that describe plastic deformations of the whole plate. These equations can be verified by modeling a plane strain shell element model in FEA. FEA might also help to describe the 3D-effects, so that a starting shape of a second cross-section is known. By using more of the possibilities with finite element software, a better description of the whole plate deformations can be found.

The 2D assumptions bring up the main discussion point in this thesis. In future work, it is recommended that an experimental validation should be performed. This would help to validate or further develop the 3D-effects. For example, it is recommended to roll and bend an example plate a couple of times. By capturing the shape, the rolling and bending forces during the actual process, the analytical model can reproduce these steps and the model can be verified. This is only possible whenever the 3D-effects are taken into account.

Elastic-perfectly plastic stress-strain curve is assumed to be sufficient for a more simple 2D simulation as performed. Residual stresses and material hardening are not taken into account in this thesis. These two topics influence the behaviour of the plate. In a future study, at least the material hardening should be taken into account. It is expected that material hardening does have an effect on the forming procedure for a complex shape with a lot of required bending operations. This also means that a more realistic stress-strain curve should be used in a future study.

The plate rolling model does have a verified force-membrane strain relationship. The relation between curvature and membrane strain needs validation or verification. A verification of this can be done by assuming a plane strain 2D-FEA model, and use a uniform pressure on different line parts. Simplifying to a press simulation is also done by Rady [23]. This should result in a uniform distribution of the membrane strain of each line part, and a global curvature.

In finding the bending procedure for the example geometry, it is concluded that the ratio between the support distance and length of cross-section has a large influence on the obtained shape. It is therefore recommended to study a larger example geometry. For such a small plate, a wider plate can be used to create an accurate shape. Hereafter, the oversized width can be trimmed.

For a future study, it is recommended to capture the total forming process of an example geometry precisely. Hereafter, the inverse forming process can be calculated analytically, and points of improvement for the process can be introduced. This means, forces and locations are used as input and the shape will be the output of the model. This definitely will give points of improvement on the analytical equations and calculated shapes.

Finally, the ultimate goal in a future study will be the optimization of the total forming process. To achieve this, the bending and rolling process need to be linked and all possible forming procedures should be considered. The forming process with the least amount of operations will finally result in the shortest forming time.

Bibliography

[1] IHC Metalix, 2021.

[2] A. Baltov and A. Sawczuk. A Rule of Anisotropic Hardening. *Acta Mechanica*, 1(2):81–92, 1965.

[3] U. Borah, S. Venugopal, R. Nagarajan, P. V. Sivaprasad, S. Venugopal, and Baldev Raj. Estimation of springback in double-curvature forming of plates: Experimental evaluation and process modeling. *International Journal of Mechanical Sciences*, 50(4):704–718, 2008.

[4] D. T. Dat and T. Peköz. *The strength of cold-formed steel columns*. PhD thesis, Cornell University, 1980.

[5] P. Dusicka, A. M. Itani, and I. G. Buckle. Cyclic response of plate steels under large inelastic strains. *Journal of Constructional Steel Research*, 63(2):156–164, 2007.

[6] G. Gadamchetty, A. Pandey, and M. Gawture. On Practical Implementation of the Ramberg-Osgood Model for FE Simulation. *SAE International Journal of Materials and Manufacturing*, 9(1): 200–205, 2016.

[7] P. J. Hancell and S. J. Harvey. The Use of Kinematic Hardening Models in Multi-Axial Cyclic Plasticity. *Fatigue of Engineering Materials and Structures Vol.*, 1:271–279, 1979.

[8] S. C. Heo, Y. H. Seo, J. W. Park, T. W. Ku, J. Kim, and B. S. Kang. Application of flexible forming process to hull structure forming. *Journal of Mechanical Science and Technology*, 24:137–140, 2010.

[9] J.H. Hollomon. Tensile Deformation. *Aime Trans*, 12(4):1–22, 1945.

[10] S. Y. Hwang and J. H. Lee. Feasibility of Multipoint Press with Continuously Divisional Forming for Double Curvature Plates in Shipbuilding. *Journal of Ship Production and Design*, 34(2):94–110, 2018.

[11] S. Y. Hwang, J. H. Lee, Y. S. Yang, and M. J. Yoo. Springback adjustment for multi-point forming of thick plates in shipbuilding. *CAD Computer Aided Design*, 42(11):1001–1012, 2010.

[12] IHC Metalix. Metal Construction Kits. URL `https://www.royalihc.com/en/products/other-industries/metal-construction-kits`.

[13] W. Johnson and T. X. Yu. On the range of applicability of results for the springback of an elastic/perfectly plastic rectangular plate after subjecting it to biaxial pure bending-II. *International Journal of Mechanical Sciences*, 23(10):631–637, 1981.

[14] W. Johnson and T. X. Yu. Springback after the biaxial elastic-plastic pure bending of a rectangular plate-I. *International Journal of Mechanical Sciences*, 23(10):619–630, 1981.

[15] R. Kwesi Nutor. Using the Hollomon Model to Predict Strain-Hardening in Metals. *American Journal of Materials Synthesis and Processing*, 2(1):1–4, 2017.

[16] M. G. Lee, S. J. Kim, and H. N. Han. Finite element investigations for the role of transformation plasticity on springback in hot press forming process. *Computational Materials Science*, 47(2): 556–567, 2009.

[17] Y. H. Lin and M. Hua. Influence of strain hardening on continuous plate roll-bending process. *International Journal of Non-Linear Mechanics*, 35(5):883–896, 2000.

[18] B. Liu, R. Villavicencio, and C. Guedes Soares. Experimental and numerical analysis of residual stresses and strains induced during cold bending of thick steel plates. *Marine Structures*, 57 (September 2017):121–132, 2018.

[19] Z. Liu, Y. Luo, Y. Wang, and T. W. Liao. A new curvature analytical method in plate leveling process. *ISIJ International*, 58(6):1094–1101, 2018.

[20] C. D. Moen, T. Igusa, and B. W. Schafer. Prediction of residual stresses and strains in cold-formed steel members. *Thin-Walled Structures*, 46(11):1274–1289, 2008.

[21] Nieland Shipbuilding Presses. Production of a saddle shaped panel, 2013. URL `https://www.youtube.com/watch?v=Xuo2XwfqV0o&t=389s`.

[22] M. H. Parsa, S. Nasher al ahkami, H. Pishbin, and M. Kazemi. Investigating spring back phenomena in double curved sheet metals forming. *Materials and Design*, 41:326–337, 10 2012.

[23] E. H. Rady. *Mechanics of Die-Less Forming of Doubly Curved Metal Shells*. PhD thesis, Massachusetts Institute of Technology, 1981.

[24] W. Ramberg and W. R. Osgood. Description of stress-strain curves by three parameters. 1943.

[25] J. N. Rodrigues Branco and C. Guedes Soares. Mapping of Shell Plates of Double Curvature Into Plane Surfaces. *Journal of Ship Production*, 21(4):248–257, 2005.

[26] C. Ryu and J. G. Shin. Optimal Approximated Unfolding of General Curved Shell Plates Based on Deformation Theory. *Journal of Manufacturing Science and Engineering, Transactions of the ASME*, 128(1):261–269, 2006.

[27] M. Salimi and F. Sassani. Modified slab analysis of asymmetrical plate rolling. *International Journal of Mechanical Sciences*, 44(9):1999–2023, 2002.

[28] A. Shakeri. Isotropic-Kinematic Cyclic Hardening Characteristics of Plate Steels. *International Journal of Steel Structures*, 17(1):19–30, 2017.

[29] W. Shen, R. Yan, S. Li, and L. Xu. Spring-back analysis in the cold-forming process of ship hull plates. *International Journal of Advanced Manufacturing Technology*, 96(5-8):2341–2354, 2018.

[30] D. S. Shim, D. Y. Yang, K. H. Kim, S. W. Chung, and M. S. Han. Practical design equations for cold roll forming of doubly curved hull plates using line array roll set. *Journal of Ship Production*, 26(3):177–186, 2010.

[31] J. G. Shin, Y. R. Choi, and H. Yim. Mechanics of Die-less Asymmetric Rolling for Fabrication of Compound Curved Plates. *Journal of Manufacturing Science and Engineering, Transactions of the ASME*, 125(4):787–793, 2003. doi: `10.1115/1.1616950`.

[32] B. Štok and M. Halilovič. Analytical solutions in elasto-plastic bending of beams with rectangular cross section. *Applied Mathematical Modelling*, 33(3):1749–1760, 2009.

[33] Subsea 7. No Title, 2019. URL `https://twitter.com/Subsea7Official/status/1114103011142438915/photo/1`.

[34] H. W. Swift. Plastic Instability Under Plane Stress. *Journal of the Mechanics and Physics of Solids*, 1(1):1–18, 1952.

[35] Yong TIAN, Yan hui GUO, Zhao dong WANG, and Guo dong WANG. Analysis of Rolling Pressure in Asymmetrical Rolling Process by Slab Method. *Journal of Iron and Steel Research International*, 16(4):22–26, 2009. URL `http://dx.doi.org/10.1016/S1006-706X(09)60055-8`.

[36] A. C. Ugural and S. K. Fenster. *Advanced Strength and Applied Elasticity*. PRENTICE HALL, 4 edition, 1981.

[37] C. C. Weng and R. N. White. Cold-Bending of Thick High-Strength Steel Plates. *Journal of Structural Engineering*, 116(1):40–54, 1990.

[38] C. C. Weng and R. N. White. Residual Stresses in Cold - Bent Thick Steel Plates. *Journal of Structural Engineering*, 116(1):24–39, 1990.